
LOVM: Language-Only Vision Model Selection

Orr Zohar
Stanford Univeristy
orrzohar@stanford.edu

Shih-Cheng Huang
Stanford Univeristy
mschuanmschuang@stanford.edu

Kuan-Chieh Wang
Stanford Univeristy
wangkual@stanford.edu

Serena Yeung
Stanford Univeristy
syyeung@stanford.edu

Abstract

Pre-trained multi-modal vision-language models (VLMs) are becoming increasingly popular due to their exceptional performance on downstream vision applications, particularly in the few- and zero-shot settings. However, selecting the best-performing VLM for some downstream applications is non-trivial, as it is dataset and task-dependent. Meanwhile, the exhaustive evaluation of all available VLMs on a novel application is not only time and computationally demanding but also necessitates the collection of a labeled dataset for evaluation. As the number of open-source VLM variants increases, there is a need for an efficient model selection strategy that does not require access to a curated evaluation dataset. This paper proposes a novel task and benchmark for efficiently evaluating VLMs' zero-shot performance on downstream applications without access to the downstream task dataset. Specifically, we introduce a new task LOVM: Language- Only Vision Model Selection, where methods are expected to perform both model selection and performance prediction based solely on a text description of the desired downstream application. We then introduced an extensive LOVM benchmark consisting of ground-truth evaluations of 35 pre-trained VLMs and 23 datasets, where methods are expected to rank the pre-trained VLMs and predict their zero-shot performance.

1 Introduction

Advancements in artificial intelligence (AI) have permeated diverse sectors, but applications in areas such as medicine or those with long-tail distributions often struggle to collect the sizable training datasets required for the standard supervised learning framework. Pre-trained vision-language models (VLMs) offer a promising solution, demonstrating robust performance on diverse downstream vision tasks without the necessity of large-scale labeled datasets [Radford et al., 2021, Jia et al., 2021]. However, the performance of VLMs can vary substantially across different tasks and domains, which undermines the reliance solely on benchmark dataset performance for effective VLM selection. Consequently, users aiming to *select a VLM* for custom downstream applications frequently face a predicament: the lack of established performance rankings for these specific, non-conventional tasks.

As the number of pre-trained VLMs increases (see Fig. 1, [Ilharco et al., 2021] and App. Tab. 4), the challenge of model selection escalates. Exhaustive evaluation of all available VLMs on a novel application is not only time and computationally demanding but also necessitates the collection of a labeled dataset for evaluation. However, many users lack the resources or technical proficiency to collect and label an evaluation dataset and subsequently evaluate all available VLMs. Consequently, the development of methods that efficiently select the most suitable model for a given task without relying on access to the downstream task dataset has become critically important.

Recent studies have demonstrated that text embeddings from VLMs can be used as a proxy for their corresponding image embeddings in various downstream tasks, including classification and error slice discovery [Zhang et al., 2023, Eyuboglu et al., 2022, Jain et al., 2022]. Specifically, although Liang et al. [2022] has shown that there exists a modality gap between text and image embeddings generated from VLMs, the geometry of this modality gap permits cross-modality transferability. This phenomenon allows text to serve as a proxy to corresponding images and vice versa. Therefore we aim to explore the utilization of cross-modality transferability to estimate VLM performance on a novel vision task using text alone.

Herein, we propose a novel problem setting - Language-Only VLM selection (LOVM) as a novel model selection task. In the LOVM task, methods are expected to select the optimal VLM and predict its expected performance given only a text description of a downstream vision task/application. (see Fig. 2). Importantly, LOVM eliminates the need to gather, organize, and annotate custom datasets, thereby greatly simplifying the model selection process for downstream users. To facilitate the development of LOVM methods in the future, we collected a large dataset of ground-truth evaluations of 35 pre-trained VLMs on 23 datasets. We then introduce the appropriate evaluation protocol and method quality metrics to allow the evaluation and comparison of LOVM methods in the future.

To show that such a challenging task is possible, we provide simple baselines that utilize readily-available large language models to generate ‘text datasets’ for a given vision task. By utilizing the cross-modality transferability phenomenon, we show how simple baselines can be derived by utilizing the cross-modality transferability phenomenon. Our results show that text prompting may be an effective means of estimating zero-shot performance, showing that such a challenging task is possible while providing a baseline for future research.

The contributions of this study can be summarized as follows:

- We propose a novel problem setting, **LOVM**: Language-Only VLM selection and performance prediction. LOVM methods are expected to perform both model selection and performance prediction using only a text description of the desired zero-shot application.
- We provide a benchmark consisting of 35 pre-trained VLMs and 23 datasets. We evaluated all dataset-VLM combinations and reported their corresponding performance, which is used as the ground truth when training and evaluating LOVM methods. We also introduce the corresponding evaluation metrics and protocols.
- In developing the LOVM baselines, we introduce several novel methodological contributions, such as using LLM models to generate text proxies for images. Our text-based methods outperform simple baselines - such as ImageNet benchmarking, showing the promise of the direction of LOVM.
- By analyzing text-based score trends, we draw insights into VLM behavior and shed light on why ResNet-based models perform better on datasets with low visual diversity.

Our code and dataset are available at <https://github.com/orrzohar/LOVM>

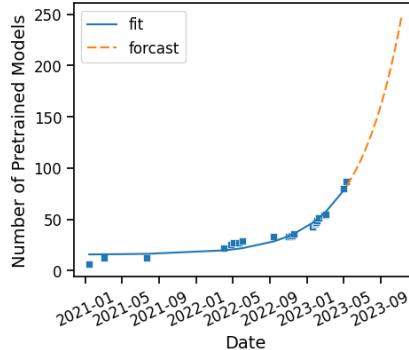


Figure 1: **LOVM Motivation.** Number of pre-trained VLMs released on openclip over time.

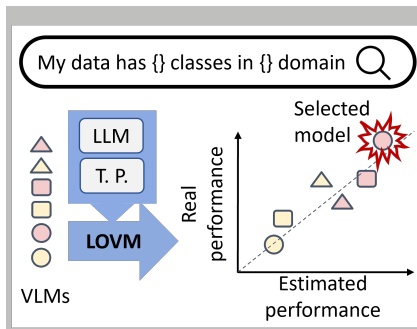


Figure 2: **An overview of an application for LOVM methods.** A user can type into a search bar the details of the desired task, and then LOVM methods evaluate and rank the available models.

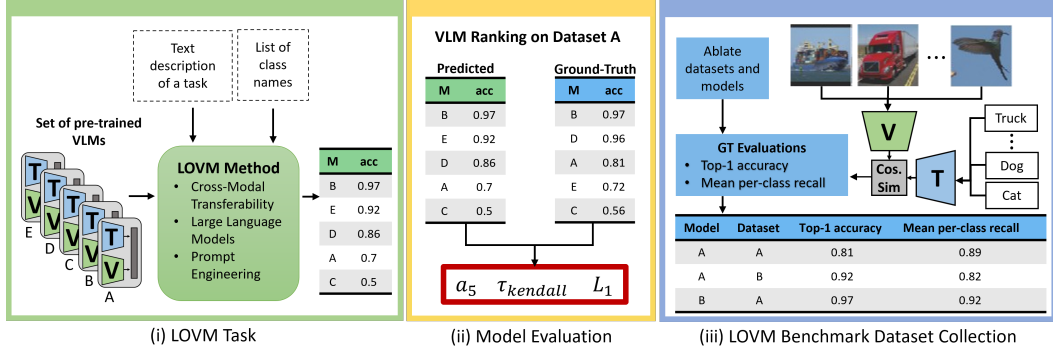


Figure 3: **Language-Only Vision Model Selection Overview.** (i) **Task.** a LOVM method is given a set of pre-trained VLMs, a text description of the desired task, and the list of the classes of interest. Given these, LOVM methods are expected to **rank and predict the performance** of all the available models on the downstream task. (ii) **Evaluation.** Given the **predicted (green)** and **ground-truth (blue)** VLM ranking and performance, we evaluate the LOVM method’s performance by accepted list ranking and accuracy metrics. (iii) **Data Collection.** We exhaustively evaluated the selected 35 VLMs on the selected 23 datasets to produce the ground-truth (image-based) evaluations.

2 Language-Only Vision Model Selection

In order to train and evaluate LOVM methods, we need the ground-truth (GT) zero-shot performance, i.e., image-based evaluation of many VLMs (differing by architecture and pre-training) on many tasks and datasets. Once collected, we can develop and evaluate LOVM methods. An ideal LOVM method should be able to select the best performing VLM for a downstream vision task and estimate the performance directly from text embeddings, eliminating the cost of image-based model selection. The VLM, dataset selection criterion, and dataset collection procedure are detailed in Sec. 2.1. Finally, the evaluation protocol of LOVM methods is described in Sec. 2.2. For a discussion on why we only evaluate zero-shot performance, see App. Sec. D.

Background. We first recap how VLMs are used as in zero-shot vision tasks. Given a pre-trained VLM v , along with an image $X \in \mathcal{X}$ or text $Y \in \mathcal{Y}$ input, we can obtain their L_2 -normalized embeddings x or y from the image encoder $f_x : \mathcal{X} \mapsto \mathbb{R}^n$ or the text encoder $f_y : \mathcal{Y} \mapsto \mathbb{R}^n$, where n is the dimension of the shared multi-modal embedding space. To use a model v on a particular task, one encodes the class prompts, Y^c for class c using the model’s text encoder, producing the class embeddings $y^c = f_y(Y^c)$. To produce the final class prediction, one calculates the cosine similarity of an image embedding with all the corresponding text embeddings to predict the class logits.

Task Definition In the LOVM task, for any downstream application/dataset d , methods are given a set of pre-trained VLMs, $\mathbf{V} = \{v_0, v_1, \dots\} \in \mathcal{V}$, a text description of the downstream task Y_d (e.g., classification) and a list of the desired class names $Y_d^c, \forall c \in C_d$ where C_d is the number of classes in task d . Given this, LOVM methods are expected to **rank and predict the accuracy** of the set of models (see Fig. 3, i):

$$p_{v,d} = f_{\text{LOVM}}(v, \{Y_d^c\}_{c=1}^{C_d}, Y_d), \quad \forall v \in \mathbf{V}, \quad (1)$$

where $p_{v,d} \in \mathbb{R}$ is the relative/absolute performance of model v on dataset d .

2.1 Data Collection

To train and evaluate LOVM methods, we need the **zero-shot** ground-truth performance of many VLM models on many downstream datasets. We, therefore, selected 35 VLMs and 23 Datasets and then performed image-based evaluations of each model on all the datasets - a total of 805 evaluations using the same prompting strategies discussed by Radford et al. [2021], See Fig. 3, iii. **These ground truth zero-shot image-based model rankings and accuracies constitute the bulk of our benchmark.** The proposed LOVM benchmark consists of the aforementioned evaluation tables as well as the per-dataset prompting templates, class names, and domain descriptions.

Selected Datasets. The proposed LOVM benchmark utilizes a heterogeneous assortment of 23 datasets. These datasets exhibit variability in the number of classes, their target tasks, and corresponding domains. The benchmark encompasses a comprehensive range of tasks such as classification, scene understanding, geolocalization, and object counting, rendering it extensively applicable across many applications. Further, the datasets span diverse domains, including natural, satellite, text, and medical images (See Tab. 1). To ensure maximal compatibility, we have opted for tasks that permit the utilization of the same VLM architecture, precluding any requisite alterations or additional training. This approach necessitated the exclusion of tasks such as segmentation and object detection, which mandate additional training modules, introducing extraneous noise during the evaluation of VLM performance.

Table 1: Details on the different datasets used, including the number of classes, tasks, and domain.

Dataset	Classes	Task	Domain
Imagenet	1000	classification	natural image
Stanford Cars	196	classification	natural image
Flowers102	102	classification	natural image
CIFAR100	100	classification	natural image
GTSRB	43	classification	natural image
VOC2007	20	classification	natural image
Oxford Pets	37	classification	natural image
STL10	10	classification	natural image
DTD	46	classification	textural image
RESISC4	45	classification	satellite images
EuroSAT	10	classification	satellite images
MNIST	10	classification	hand-writing
Retinopathy	5	classification	retina scan
PCam	2	classification	histopathology
SUN397	397	scene und.	natural image
Country211	211	geolocation	natural image
SVHN	10	OCR	natural image
CLEVR-C	8	object counting	natural image
CLEVR-D	8	distance est.	natural image
DMLab	6	distance est.	synthetic
FER2013	7	fac. exp. rec.	natural image
KITTI	4	distance est.	natural image
Rendered SST2	2	OCR	text image

VLM Model Candidates. We utilize the open-clip library [Ilharco et al., 2021], a diverse collection of pre-trained VLMs spanning various architectures, including but not limited to CLIP and CoCa models, and utilizing encoders such as ResNet, ConvNext, and ViT. These models have undergone pre-training on various datasets, such as WIT [Radford et al., 2021], LAION 400m, and LAION 2b [Schuhmann et al., 2022], with different hyperparameters. From the 87 models currently available, we have carefully selected 35 for our study. A comprehensive list of all models used in this benchmark can be found in the App. Tab. 4. We avoided incorporating additional multi-modal models, such as BEIT [Wang et al., 2023] and VLMO [Bao et al., 2022], as these models utilize a shared text-image encoder and, therefore, cannot be evaluated on the same datasets as CoCa and CLIP. Utilizing models from the open-clip library ensures maximum compatibility and reproducibility in our work. Currently, CLIP models comprise a significant portion of VLMs employed in practice.

2.2 LOVM Evaluation Protocol

On our benchmark, methods are expected to rank 35 pre-trained multi-modal models that differ in architecture and pre-training datasets on 23 target datasets, and compare these rankings to the ground-truth rankings (see Fig. 3 (ii)) and report the performance for each of the 23 datasets as well as their averaged values.

Model Ranking. When evaluating model ranking on a particular dataset, one has access to the performance of all the models on all the datasets besides the one being evaluated. We use the following metrics:

- *Top-5 Recall (R_5)* – We used R_5 to evaluate a LOVM method’s model ranking capability. It is defined as the ratio of correctly identified models.
- *Kendall’s Rank Correlation (τ)* – We used τ to evaluate a LOVM method’s model selection capability and give a fine-grained picture of how well the method ranked the high-performing models and is defined as Kendall’s rank over the top-5 selected models.

Performance Prediction. When evaluating a model’s prediction on a dataset, the GT performance of that model on all datasets and the performance of all models on that dataset are held out.

- *Mean Absolute Error (L_1)* – We used L_1 to evaluate a LOVM method’s performance prediction capability. Specifically, we compute the L_1 loss of all models’ predicted vs. actual mean per-class recall/top-1 accuracy.

3 LOVM Baselines

The assessment of model performance in traditional supervised methods often relies on benchmark dataset performance. Given that most pre-trained vision-language models (VLMs) are evaluated on ImageNet, it is convenient to utilize it as a baseline for comparison (This is our ImageNet Benchmark baseline). Alternatively, a large language model could generate many probable image captions, which could be encoded using the different VLMs text encoder, producing the corresponding text embeddings. Treating these embeddings as image-proxies, one can calculate different widely-accepted scores (see Sec. 3.2) and fit a linear regression model to predict performance or rank VLMs. Specifically, from every VLM-dataset combination, one extracts these scores and then fits the model:

$$p_{v,d} = \mathbf{w} \cdot \mathbf{s}_{v,d} + b, \tag{2}$$

$$s_{v,d}^i = f_{\text{feat}}^i(v, \text{TextGen}(\{Y_d^c\}_{c=1}^{C_d}, Y_d)), \tag{3}$$

where $p_{v,d} \in \mathbb{R}$ is the relative/absolute performance of model v on dataset d , \mathbf{w}, b are the weights and bias of the linear model. $s_{v,d}^i$ is the i -th element in the score vector, $\mathbf{s}_{v,t} = [s_{v,d}^1, s_{v,d}^2, \dots]^T$, produced by the corresponding feature/score function f_{feat}^i . The function `TextGen` is a function that generates text given the class names, $\{Y_d^c\}_{c=1}^{C_d}$ and task description Y_d of the desired task/dataset d . We discuss the different scores, $s_{v,d}^i$, in Sec. 3.2 and the `TextGen` function in Sec. 3.1. To evaluate model rankings on a dataset, we hold out the data for that particular dataset and fit a linear model on all the other datasets. Meanwhile, to evaluate the performance prediction of some model on a particular dataset, we hold out the data for that dataset and model and fit a linear model on the remaining combinations. We refer to the baselines by the combination of scores used in the linear model.

3.1 Text Data Generation

The impressive progress in large language models (LLMs) [OpenAI, 2023, Touvron et al., 2023] has rendered the generation of potential - and realistic - ‘image captions’ practically limitless, thus rendering text data generation remarkably attainable. In our study, we employ GPT-3.5, tasked to produce two distinct text-based datasets, each corresponding to a given vision task. These generated datasets serve as the foundation for extracting essential features for our task.

Captions Dataset. To generate the captions dataset, D^{cap} , we prompt an LLM to generate realistic - but confusing - captions for images containing the user-provided classes in the user-provided domain. We extracted the dataset description and class names from each dataset and prompted the LLM:

Generate long and confusing image captions for the {domain} domain, which will be used to evaluate a Vision-Language Model’s {task} performance.
Generate 50 captions for {classname}:

Where we assume the user supplies the target domain and task description. For examples of different dataset’s domain and task, see Tab. 3.

Synonyms Dataset. Prior studies have already leveraged synonyms to evaluate LLMs [van der Lee et al., 2022]. For example, if an LVM has seen many instances of the class ‘chair’ referenced as a ‘chair’, ‘seat’, etc., we expect these embeddings to be closely located in the shared embedding space. To evaluate this aspect of the VLM using text, we prompt an LLM to generate a list of semantically similar/synonyms for every object class. For example, for the class “chair”, we get: “seat”, “bench”, “armchair”, and “furniture”. We prompt the LLM with the following:

Please list the superclasses/synonyms for {classname}. For example:
chair: [furniture, seat, bench, armchair, sofa]
{classname}:

We collect the results from this prompt to form the synonyms dataset, D^{syn} .

Table 2: **LOVM Benchmark.** We evaluate our method’s performance over 23 datasets and 35 pre-trained models, and when predicting the top-1 accuracy and mean per-class recall (averaged over all datasets, for the per-dataset breakdown, see App. Tab. 5 and 6). INB - ImageNet Baseline, C - Text Classification scores, G - Granularity scores. As can be seen, mixed approaches achieve the best VLM ranking and performance prediction.

used scores	mean per-class recall			top-1 accuracy		
	$R_5(\uparrow)$	$\tau(\uparrow)$	$L_1(\downarrow)$	$R_5(\uparrow)$	$\tau(\uparrow)$	$L_1(\downarrow)$
INB	0.504	0.186	0.228	0.452	0.177	0.220
C	0.252	0.058	0.182	0.226	0.058	0.176
G	0.270	-0.014	0.145	0.252	-0.014	0.143
G+C	0.261	0.101	0.145	0.252	-0.014	0.143
INB+C	0.522	0.214	0.182	0.461	0.223	0.176
INB+G	0.539	0.197	0.145	0.461	0.096	0.141
INB+G+C	0.539	0.197	0.145	0.461	0.223	0.141

3.2 Text-Derived Scores

There are many widely reported metrics for model transferability, dataset difficulty, and dataset granularity scores developed on image embeddings. We extract different commonly used features/metrics from the text dataset embeddings and calculate their text-only counterparts.

Text Classification Scores (C). We use the generated captions dataset as image proxies and evaluate the resulting model performance. Specifically, we replace the images with the generated image captions and evaluate each model’s text top-1 accuracy, **text-acc1** and f1-score **text-f1**.

Dataset Granularity Scores (G). Cui et al. [2019] introduced the use of two widely used dataset granularity measures for image classification, Fisher criterion [Fisher, 1936], ϕ_{fisher} and Silhouette score [Rousseeuw, 1987], φ_{sil} , and their normalization constant, Class Dispersion score, ρ_{disp} . The Fisher criterion measures the degree of similarity of the classes or the extent of their separation. The Silhouette score is a well-established metric used to quantify the tightness of the same-class samples to the separation of different-class samples. The Class Dispersion score quantifies the degree of same-class tightness or data cone radius.

Recently, van der Lee et al. [2022] has shown that synonym consistency can be used in large language models to correlate the degree of familiarity of the model with a particular concept. Using the Synonym dataset, we compare the cosine similarity between the text embedding of each class and its corresponding synonyms. A high Synonym Consistency score, γ_{syn} , between the class and its corresponding synonyms indicates that the model is aware of the semantic meaning of the class.

For detailed definitions of these metrics, see App. Sec. B.

4 Experiments and Results

In Sec. 4.1, we evaluate the model selection capabilities of the proposed baselines on the LOVM benchmark. In Sec. 4.2, we evaluate the proposed baselines performance prediction capabilities. We then analyse score trends and draw insights in Sec. 4.3.

4.1 Model Selection

A core aspect of this benchmark is model selection, as it allows the user to quickly and easily select the optimal model for the desired downstream task. From Tab. 2, we can see that, when predicting/ranking by the models mean per-class recall, the (C+G)-baseline can achieve a top-5 recall of 0.261, indicating that, on average, more than one model is correctly ranked as a top-5 performing model. Meanwhile, the INB-baseline had a R_5 of 0.505. Combining the text and ImageNet scores, the (INB+G)-baseline achieves the highest accuracy of 0.539, a $\sim 15\%$ improvement over the INB-baseline. When studying Kendall’s rank correlation, the (G+C)-, INB-, and (INB+G)-baselines achieve a τ of 0.101, 0.186, and

0.214, respectively. The (INB+G)-baseline had the highest rank correlation with $\sim 6\%$ improvement over the INB-baseline. Similar results can be seen when predicting the top-1 accuracy. The consistent improvement of the baselines over the INB-baseline indicates the utility of both text-based and benchmark features. Interestingly, C-score (or the text-acc1) appears to be more influential in predicting/ranking model’s the top-1 accuracy than the mean per-class recall.

4.2 Performance Prediction

Based on Tab. 2, it is clear that the granularity scores (G) are instrumental to predicting a model’s top-1 accuracy and mean per-class recall. The G-baseline approach can achieve an average L_1 error of 0.145 and 0.141 for predicting the mean-per-class recall and top-1 accuracy, respectively. Adding any other scores does not lead to an improvement in performance prediction. The INB-baseline, which uses Imagenet performance as prediction, leads to a much higher L_1 error of 0.228 and 0.220 compared to the text-base baselines (text-based performance estimation outperformed INB-baselines by $\sim 36\%$). Finally, adding the ImageNet benchmark score to the text features in the Unified baseline did not improve the L_1 compared to the text-only baseline. This is expected as the imagenet performance cannot be used to predict the performance on a different dataset. Fig. 4 shows the predicted vs. ground-truth accuracy. Our approach had a R^2 score (or coefficient of determination) of $= 0.55$, showing significant room for improvement in accuracy prediction.

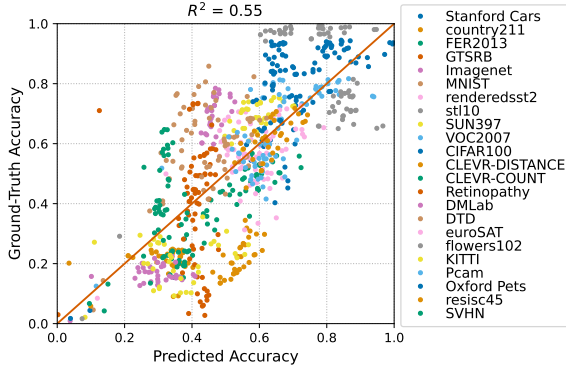


Figure 4: **Predicted vs. Ground-Truth Accuracy.** Predicted vs. actual top-1 accuracy on the proposed LOVM benchmark.

4.3 Insights into VLM Behavior

In this section, we visualize the dependence of the text-derived features on the pre-training datasets and model architectures while averaging them across the different datasets (see Fig. 5).

Model Size. From studying Fig. 5, we can identify a clear trend of Fisher criterion and Silhouette score improving with model size, while Class Dispersion score and Synonym Consistency score degrade with model size. Silhouette score quantifies the degree of inter-class overlap or the degree of overlap between different classes in the embedding space. As the model size of the visual encoder increases, the embeddings from different classes become more and more orthogonal, decreasing the inter-class overlap. Fisher criterion quantifies the degree of granularity a model perceives the target datasets to be. As model size decreases, Fisher criterion decreases, or the degree of perceived granularity increases. Class Dispersion score quantifies the degree of intra-class dispersion, or how similar embeddings of the same class are. Specifically, as we increase model size, Class Dispersion score decreases, and therefore the class embeddings become more varied, effectively expanding the class cone radius. Synonym Consistency score quantified the closeness of a class to its synonyms and behaved similarly to Fisher criterion.

Pre-training Dataset. When studying the effect of pre-training dataset size, it is clear that there is a positive correlation between pre-training dataset size and all of the metrics when comparing models of the same size. As the pre-training dataset increases, the intra-class similarity increases more rapidly than the inter-class similarity, hence effectively different classes are more separated. Specifically, Fisher criterion and Silhouette score increase, or the degree of perceived granularity decreases, and embeddings from different classes become less orthogonal, increasing the inter-class overlap. As the pre-training dataset size increases, Class Dispersion score increases and the intra-class dispersion is more condensed, leading to a smaller effective radius of a class dataset cone. Interestingly, larger models are more affected by the increase in dataset size (as seen by the large slope of ViT-L compared

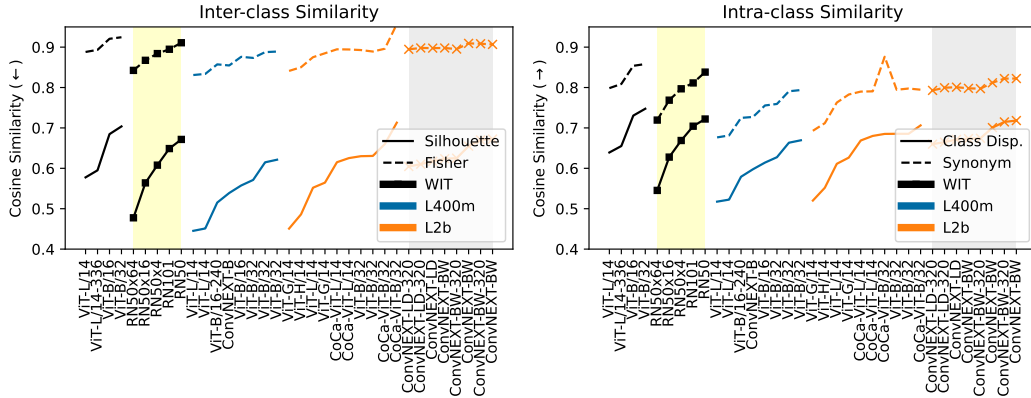


Figure 5: **Analyzing Score Trends.** Average text scores dependence on pre-training datasets and model architecture on our text-derived scores. (left) scores quantifying inter-class similarity (right) scores quantifying intra-class similarity. ResNet (■) and ConvNext (×) based models are grouped separately to evaluate their effect on the score trends.

to ViT-B) - which could explain previous works’ observation that larger models benefit more when trained on larger datasets [Fang et al., 2022].

Model Architecture. Pre-training datasets and model architectures significantly influence each other. ResNets and ViTs, for instance, consistently demonstrated differing behaviors and appeared to reside at distinct points on the class separation-dispersion trade-off curve. In particular, ResNets displayed lower Class Dispersion score and Silhouette score, indicating challenges in encoding instances of the same class within the feature space compared to ViTs. This may account for ResNets’ superior performance on datasets with low visual variation, like MNIST; as the visual variation is relatively low, we would not expect the Class Dispersion score to be the limiting factor in model performance, making them less affected by this aspect of the dataset. Intriguingly, ConvNEXT models exhibited characteristics more in line with ViT-base models than ResNet-based ones. What leads to variation between WIT and L400m remains unclear, necessitating further investigation.

5 Related Work

Vision-Language Models. The field of vision-language models (VLMs) has witnessed significant progress in recent years, particularly with the introduction of contrastive pre-trained VLMs such as CLIP [Radford et al., 2021]. These models leverage large-scale datasets of aligned image-caption pairs to obtain shared embedding spaces that capture rich visual and textual features. The learned image and text encoders from these VLMs have demonstrated impressive feature extraction capabilities and even set state-of-the-art zero-shot performances. However, the performance of VLMs can vary significantly across different datasets, especially when there exists a domain, content, or distribution shift [Fang et al., 2022]. As the number of model architectures & pre-training datasets [Ilharco et al., 2021, Schuhmann et al., 2022] increase, it is challenging to select a pre-trained VLM, as good performance on existing benchmarks does not always translate to the downstream task. Therefore, there is a need to develop strategies that can estimate VLM performance on a new task without requiring an exhaustive evaluation of these models using the target dataset.

Text as a Proxy For Images. While these VLMs aim to project representations from different modalities into a shared embedding space, Liang et al. [2022] found that corresponding image and text pairs don’t completely overlap in the embedding space. Instead, a “modality gap” exists between the image embeddings and text embeddings sub-space. Subsequently, Zhang et al. [2023] has found that this gap can be approximated as an orthogonal constant between true pairs of image and text and is, therefore, parallel to the decision boundaries for a given modality. This suggests that cross-modality transferability - using one modality as input to the other’s classifier - is possible for these contrastively pre-trained VLMs. Several studies have demonstrated the utility of the cross-modality transferability

phenomenon in different tasks. For instance, Domino leveraged the cross-modal embeddings to identify error slices and generate natural language descriptions of the error slices [Eyuboglu et al., 2022]. Similarly, Jain et al. [2022] used these embeddings to discover model failure directions in the multi-modal embedding space. Meanwhile, Zhang et al. [2023] proposed the DrML, which diagnoses and rectifies vision classifiers using natural language inputs. In this study, we also use text as a proxy for images, but for the novel task of ranking and estimating VLM performance.

Unsupervised Model Selection. Unsupervised model selection was recently introduced by Sun et al. [2021], to select the best model for a new target domain without utilizing labeled data. Their work only considered domain (and not content) shifts and proposed constructing a proxy dataset that captures/closely approximates this shift. This proxy dataset is constructed by minimizing different dataset statistics using several labeled datasets. Evaluating models on this proxy set performs well for model selection/ranking. However, such a strategy is limiting in the setting of evaluating VLMs - the size of these models and their pre-training datasets makes it too computationally expensive to achieve the desired goal of evaluating model performance on *any* downstream task.

Unsupervised Accuracy Estimation. Unsupervised or label-free accuracy estimation aims to estimate classifier model performance with only access to the unlabeled test set of a new task. Platanios et al. [2017, 2016] proposed strategies to apply probabilistic modeling approaches, such as the probabilistic logic or Bayesian modeling, to analyze and aggregate predictions from multiple classifiers. Other works approach this task by fitting models on feature statistics of the target dataset [Risser-Maroux and Chamand, 2023]. Some studies evaluated model agreement, where many classifiers are used on the target dataset, and the degree of agreement was correlated with model performance [Chen et al., 2021, Jiang et al., 2022]. Other approaches for unsupervised accuracy estimation include training a neural network on the weight distribution statistics [Unterthiner et al., 2020] or composing a meta-dataset with available datasets, such that the meta-dataset matched some target dataset statistics [Deng and Zheng, 2021]. Some have attempted to craft embedding-based scores, trying to quantify the separability of clusters in the embeddings spaces [Pándy et al., 2022, Ding et al., 2022]. All these methods assume access to the unlabeled dataset of the target task. Instead, our method only requires text descriptions of the novel task to estimate the model’s performance.

6 Conclusion

In this work, we introduce a new problem setting and task LOVM, which aims to select the best-performing VLMs for a downstream vision task by only using its textual description. To demonstrate the feasibility of such a task, we show how large language models, in combination with the cross-modal transferability phenomenon, can be leveraged for such a task. We exhaustively test these methods on the proposed LOVM benchmark, consisting of 35 VLMs and 23 benchmark datasets. Our findings validate the viability of our proposed LOVM task, with unified (both text scores and ImageNet benchmarking) baselines outperforming the ImageNet benchmarking baseline. This suggests that text-based model selection methods (i.e., LOVM methods) provide additional benefits to baseline selection based on a model’s performance on ImageNet. Furthermore, we found that the granularity-based scores influence performance prediction and modal ranking more greatly. These findings bolster the research direction of developing methods for VLM selections using only text.

Our proposed LOVM benchmark aims to foster this research direction. We see two promising avenues for future research: (i) improving text-based classification correlation with ground-truth accuracy by either text generation, evaluation metrics, or cross-modal transferability, and (ii) introducing new granularity and transferability scores to the text-only paradigm. Namely, we anticipate the development of methods improving over our proposed baselines presented in Tab. 2. Our work aims to facilitate future research in this area and provide a more accurate and reliable means of comparing pre-trained VLMs, accelerating their utilization in downstream applications.

For a discussion about broader and potential negative societal impacts please see App. Sec E.

Acknowledgments. We gratefully acknowledge the computational credits provided by Google Cloud Platform through Stanford’s HAI Institute for Human-Centered Artificial Intelligence. We also thank the Knight-Hennessy Scholars Foundation for generously funding Orr Zohar.

References

- Andrea Agostinelli, Michal Pándy, Jasper Uijlings, Thomas Mensink, and Vittorio Ferrari. How stable are transferability metrics evaluations? In Shai Avidan, Gabriel Brostow, Moustapha Cissé, Giovanni Maria Farinella, and Tal Hassner, editors, *Computer Vision – ECCV 2022*, pages 303–321, Cham, 2022. Springer Nature Switzerland. ISBN 978-3-031-19830-4.
- Hangbo Bao, Wenhui Wang, Li Dong, Qiang Liu, Owais Khan Mohammed, Kriti Aggarwal, Subhojit Som, Songhao Piao, and Furu Wei. VLMo: Unified vision-language pre-training with mixture-of-modality-experts. In *Advances in Neural Information Processing Systems*, 2022. URL <https://openreview.net/forum?id=bydKs84JEyw>.
- Jiefeng Chen, Frederick Liu, Besim Avci, Xi Wu, Yingyu Liang, and Somesh Jha. Detecting errors and estimating accuracy on unlabeled data with self-training ensembles. *Advances in Neural Information Processing Systems*, 34:14980–14992, 2021.
- Gong Cheng, Junwei Han, and Xiaoqiang Lu. Remote sensing image scene classification: Benchmark and state of the art. *Proceedings of the IEEE*, 105(10):1865–1883, Oct 2017. ISSN 1558-2256. doi: 10.1109/jproc.2017.2675998. URL <http://dx.doi.org/10.1109/JPROC.2017.2675998>.
- M. Cimpoi, S. Maji, I. Kokkinos, S. Mohamed, and A. Vedaldi. Describing textures in the wild. In *Proceedings of the IEEE Conf. on Computer Vision and Pattern Recognition (CVPR)*, 2014.
- Adam Coates, Andrew Ng, and Honglak Lee. An analysis of single-layer networks in unsupervised feature learning. In *Proceedings of the fourteenth international conference on artificial intelligence and statistics*, pages 215–223. JMLR Workshop and Conference Proceedings, 2011.
- Yin Cui, Zeqi Gu, Dhruv Mahajan, Laurens van der Maaten, Serge Belongie, and Ser-Nam Lim. Measuring dataset granularity, 2019. URL <https://arxiv.org/abs/1912.10154>.
- Jia Deng, Wei Dong, Richard Socher, Li-Jia Li, Kai Li, and Li Fei-Fei. Imagenet: A large-scale hierarchical image database. In *2009 IEEE conference on computer vision and pattern recognition*, pages 248–255. Ieee, 2009.
- Weijian Deng and Liang Zheng. Are labels always necessary for classifier accuracy evaluation? In *Proceedings of the IEEE/CVF Conference on Computer Vision and Pattern Recognition (CVPR)*, pages 15069–15078, June 2021.
- Nan Ding, Xi Chen, Tomer Levinboim, Soravit Changpinyo, and Radu Soricut. Pactran: Pac-bayesian metrics for estimating the transferability of pretrained models to classification tasks. In Shai Avidan, Gabriel Brostow, Moustapha Cissé, Giovanni Maria Farinella, and Tal Hassner, editors, *ECCV 2022*, pages 252–268, Cham, 2022. Springer Nature Switzerland. ISBN 978-3-031-19830-4.
- Yoshua Bengio Dumitru Ian Goodfellow, Will Cukierski. Challenges in representation learning: Facial expression recognition challenge, 2013.
- Kawin Ethayarajh, Yejin Choi, and Swabha Swayamdipta. Understanding dataset difficulty with \mathcal{V} -usable information, 2021. URL <https://arxiv.org/abs/2110.08420>.
- M. Everingham, L. Van Gool, C. K. I. Williams, J. Winn, and A. Zisserman. The PASCAL Visual Object Classes Challenge 2007 (VOC2007) Results. <http://www.pascal-network.org/challenges/VOC/voc2007/workshop/index.html>, 2007.
- Sabri Eyuboglu, Maya Varma, Khaled Kamal Saab, Jean-Benoit Delbrouck, Christopher Lee-Messer, Jared Dunnmon, James Zou, and Christopher Re. Domino: Discovering systematic errors with cross-modal embeddings. In *International Conference on Learning Representations*, 2022. URL <https://openreview.net/forum?id=FPCMqjI0jXN>.
- Alex Fang, Gabriel Ilharco, Mitchell Wortsman, Yuhao Wan, Vaishaal Shankar, Achal Dave, and Ludwig Schmidt. Data determines distributional robustness in contrastive language image pre-training (clip), 2022. URL <https://arxiv.org/abs/2205.01397>.

- Leo Feng, Mohamed Osama Ahmed, Hossein Hajimirsadeghi, and Amir Abdi. Towards better selective classification, 2022. URL <https://arxiv.org/abs/2206.09034>.
- Ronald A Fisher. The use of multiple measurements in taxonomic problems. *Annals of eugenics*, 7 (2):179–188, 1936.
- Andreas Geiger, Philip Lenz, Christoph Stiller, and Raquel Urtasun. Vision meets robotics: The kitti dataset. *International Journal of Robotics Research (IJRR)*, 2013.
- Patrick Helber, Benjamin Bischke, Andreas Dengel, and Damian Borth. Eurosat: A novel dataset and deep learning benchmark for land use and land cover classification. *IEEE Journal of Selected Topics in Applied Earth Observations and Remote Sensing*, 2019.
- Gabriel Ilharco, Mitchell Wortsman, Ross Wightman, Cade Gordon, Nicholas Carlini, Rohan Taori, Achal Dave, Vaishaal Shankar, Hongseok Namkoong, John Miller, Hannaneh Hajishirzi, Ali Farhadi, and Ludwig Schmidt. Openclip, July 2021. URL <https://doi.org/10.5281/zenodo.5143773>.
- Saachi Jain, Hannah Lawrence, Ankur Moitra, and Aleksander Madry. Distilling model failures as directions in latent space, 2022. URL <https://arxiv.org/abs/2206.14754>.
- Chao Jia, Yinfei Yang, Ye Xia, Yi-Ting Chen, Zarana Parekh, Hieu Pham, Quoc V. Le, Yun-Hsuan Sung, Zhen Li, and Tom Duerig. Scaling up visual and vision-language representation learning with noisy text supervision. *CoRR*, abs/2102.05918, 2021. URL <https://arxiv.org/abs/2102.05918>.
- Yiding Jiang, Vaishnavh Nagarajan, Christina Baek, and J Zico Kolter. Assessing generalization of SGD via disagreement. In *International Conference on Learning Representations*, 2022. URL <https://openreview.net/forum?id=WvOGCEAQhx1>.
- Justin Johnson, Bharath Hariharan, Laurens Van Der Maaten, Li Fei-Fei, C Lawrence Zitnick, and Ross Girshick. Clevr: A diagnostic dataset for compositional language and elementary visual reasoning. In *Proceedings of the IEEE conference on computer vision and pattern recognition*, pages 2901–2910, 2017.
- Kaggle and EyePacs. Kaggle diabetic retinopathy detection, 2015. URL <https://www.kaggle.com/c/diabetic-retinopathy-detection/data>.
- Jonathan Krause, Michael Stark, Jia Deng, and Li Fei-Fei. 3d object representations for fine-grained categorization. In *4th International IEEE Workshop on 3D Representation and Recognition (3dRR-13)*, Sydney, Australia, 2013.
- Alex Krizhevsky, Geoffrey Hinton, et al. Learning multiple layers of features from tiny images, 2009.
- Yann LeCun, Corinna Cortes, and CJ Burges. Mnist handwritten digit database. *ATT Labs [Online]*. Available: <http://yann.lecun.com/exdb/mnist>, 2, 2010.
- Weixin Liang, Yuhui Zhang, Yongchan Kwon, Serena Yeung, and James Zou. Mind the gap: Understanding the modality gap in multi-modal contrastive representation learning. In *NeurIPS*, 2022. URL <https://openreview.net/forum?id=S7Evzt9uit3>.
- Yuval Netzer, Tao Wang, Adam Coates, Alessandro Bissacco, Bo Wu, and Andrew Y. Ng. Reading digits in natural images with unsupervised feature learning. In *NIPS Workshop on Deep Learning and Unsupervised Feature Learning*, 2011.
- Maria-Elena Nilsback and Andrew Zisserman. Automated flower classification over a large number of classes. In *Indian Conference on Computer Vision, Graphics and Image Processing*, Dec 2008.
- OpenAI. Gpt-4 technical report, 2023.
- Michal Pándy, Andrea Agostinelli, Jasper Uijlings, Vittorio Ferrari, and Thomas Mensink. Transferability estimation using bhattacharyya class separability. In *Proceedings of the IEEE/CVF Conference on Computer Vision and Pattern Recognition (CVPR)*, pages 9172–9182, June 2022.

- Omkar M. Parkhi, Andrea Vedaldi, Andrew Zisserman, and C. V. Jawahar. Cats and dogs. In *IEEE Conference on Computer Vision and Pattern Recognition*, 2012.
- Emmanouil Platanios, Hoifung Poon, Tom M Mitchell, and Eric J Horvitz. Estimating accuracy from unlabeled data: A probabilistic logic approach. In I. Guyon, U. Von Luxburg, S. Bengio, H. Wallach, R. Fergus, S. Vishwanathan, and R. Garnett, editors, *Advances in Neural Information Processing Systems*, volume 30. Curran Associates, Inc., 2017. URL <https://proceedings.neurips.cc/paper/2017/file/95f8d9901ca8878e291552f001f67692-Paper.pdf>.
- Emmanouil Antonios Platanios, Avinava Dubey, and Tom Mitchell. Estimating accuracy from unlabeled data: A bayesian approach. In Maria Florina Balcan and Kilian Q. Weinberger, editors, *Proceedings of The 33rd International Conference on Machine Learning*, volume 48 of *Proceedings of Machine Learning Research*, pages 1416–1425. New York, New York, USA, 20–22 Jun 2016. PMLR. URL <https://proceedings.mlr.press/v48/platanios16.html>.
- Michal Pándy, Andrea Agostinelli, Jasper Uijlings, Vittorio Ferrari, and Thomas Mensink. Transferability estimation using bhattacharyya class separability. In *2022 IEEE/CVF Conference on Computer Vision and Pattern Recognition (CVPR)*, pages 9162–9172, 2022. doi: 10.1109/CVPR52688.2022.00896.
- Alec Radford, Jong Wook Kim, Chris Hallacy, Aditya Ramesh, Gabriel Goh, Sandhini Agarwal, Girish Sastry, Amanda Askell, Pamela Mishkin, Jack Clark, Gretchen Krueger, and Ilya Sutskever. Learning transferable visual models from natural language supervision. *CoRR*, abs/2103.00020, 2021. URL <https://arxiv.org/abs/2103.00020>.
- Olivier Risser-Maroux and Benjamin Chamand. What can we learn by predicting accuracy? In *Proceedings of the IEEE/CVF Winter Conference on Applications of Computer Vision (WACV)*, pages 2390–2399, January 2023.
- Peter J. Rousseeuw. Silhouettes: A graphical aid to the interpretation and validation of cluster analysis. *Journal of Computational and Applied Mathematics*, 20:53–65, 1987. ISSN 0377-0427. doi: [https://doi.org/10.1016/0377-0427\(87\)90125-7](https://doi.org/10.1016/0377-0427(87)90125-7). URL <https://www.sciencedirect.com/science/article/pii/0377042787901257>.
- Florian Scheidegger, Roxana Istrate, Giovanni Mariani, Luca Benini, Costas Bekas, and Cristiano Malossi. Efficient image dataset classification difficulty estimation for predicting deep-learning accuracy, 2018. URL <https://arxiv.org/abs/1803.09588>.
- Christoph Schuhmann, Romain Beaumont, Richard Vencu, Cade W Gordon, Ross Wightman, Mehdi Cherti, Theo Coombes, Aarush Katta, Clayton Mullis, Mitchell Wortsman, Patrick Schramowski, Srivatsa R Kundurthy, Katherine Crowson, Ludwig Schmidt, Robert Kaczmarczyk, and Jenia Jitsev. LAION-5b: An open large-scale dataset for training next generation image-text models. In *Thirty-sixth Conference on Neural Information Processing Systems Datasets and Benchmarks Track*, 2022. URL <https://openreview.net/forum?id=M3Y74vmsMcY>.
- Johannes Stallkamp, Marc Schlipsing, Jan Salmen, and Christian Igel. The german traffic sign recognition benchmark: a multi-class classification competition. In *The 2011 international joint conference on neural networks*, pages 1453–1460. IEEE, 2011.
- Xiaoxiao Sun, Yunzhong Hou, Weijian Deng, Hongdong Li, and Liang Zheng. Ranking models in unlabeled new environments. In *Proceedings of the IEEE/CVF International Conference on Computer Vision*, pages 11761–11771, 2021.
- Hugo Touvron, Thibaut Lavril, Gautier Izacard, Xavier Martinet, Marie-Anne Lachaux, Timothée Lacroix, Baptiste Rozière, Naman Goyal, Eric Hambro, Faisal Azhar, Aurelien Rodriguez, Armand Joulin, Edouard Grave, and Guillaume Lample. Llama: Open and efficient foundation language models, 2023. URL <https://arxiv.org/abs/2302.13971>.
- Thomas Unterthiner, Daniel Keysers, Sylvain Gelly, Olivier Bousquet, and Ilya Tolstikhin. Predicting neural network accuracy from weights, 2020. URL <https://arxiv.org/abs/2002.11448>.

- Chris van der Lee, Thiago Castro Ferreira, Chris Emmerly, Travis Wiltshire, and Emiel Krahmer. Neural data-to-text generation based on small datasets: Comparing the added value of two semi-supervised learning approaches on top of a large language model, 2022. URL <https://arxiv.org/abs/2207.06839>.
- Bastiaan S Veeling, Jasper Linmans, Jim Winkens, Taco Cohen, and Max Welling. Rotation equivariant CNNs for digital pathology, June 2018.
- Wenhui Wang, Hangbo Bao, Li Dong, Johan Bjorck, Zhiliang Peng, Qiang Liu, Kriti Aggarwal, Owais Khan Mohammed, Saksham Singhal, Subhojit Som, and Furu Wei. Image as a foreign language: BEiT pretraining for vision and vision-language tasks. In *Proceedings of the IEEE/CVF Conference on Computer Vision and Pattern Recognition*, 2023.
- Lauren J. Wong, Sean McPherson, and Alan J. Michaels. Assessing the value of transfer learning metrics for rf domain adaptation, 2022.
- J. Xiao, J. Hays, K. A. Ehinger, A. Oliva, and A. Torralba. Sun database: Large-scale scene recognition from abbey to zoo. In *2010 IEEE Computer Society Conference on Computer Vision and Pattern Recognition*, pages 3485–3492, June 2010. doi: 10.1109/CVPR.2010.5539970.
- Xiaohua Zhai, Joan Puigcerver, Alexander Kolesnikov, Pierre Ruysen, Carlos Riquelme, Mario Lucic, Josip Djolonga, Andre Susano Pinto, Maxim Neumann, Alexey Dosovitskiy, Lucas Beyer, Olivier Bachem, Michael Tschannen, Marcin Michalski, Olivier Bousquet, Sylvain Gelly, and Neil Houlsby. A large-scale study of representation learning with the visual task adaptation benchmark, 2020.
- Yuhui Zhang, Jeff Z HaoChen, Shih-Cheng Huang, Kuan-Chieh Wang, James Zou, and Serena Yeung. Diagnosing and rectifying vision models using language. *arXiv preprint arXiv:2302.04269*, 2023.

LOVM: Language-Only Vision Model Selection Appendix

Table of Contents

A LOVM Benchmark Details	14
A.1 LOVM Benchmark - Datasets	14
A.2 LOVM Benchmark - Vision-Language Models	14
A.3 LOVM Benchmark - Ground-Truth Model Ranking	15
B Baseline Details	15
B.1 Prompting Templates	15
B.2 Text-Derived Scores	17
B.3 Text Dataset Generation	18
B.4 Text Classification and Noise Corruption	19
C Additional Results	19
C.1 LOVM Per-Dataset Breakdown	19
C.2 Ablation Experiments	20
C.3 Raw Model Ranking Details	23
C.4 Domain Shift Experiment	24
D Limitations	26
E Broader Impacts	28

A LOVM Benchmark Details

We evaluated 35 on 23, a total of 805 evaluations. This constituted the bulk of our compute with a total of 4 days on an nvidia V100 instance. Evaluations were carried out using the CLIP_benchmark repository (https://github.com/LAION-AI/CLIP_benchmark).

A.1 LOVM Benchmark - Datasets

The proposed LOVM benchmark comprises of 23 datasets, which were selected to maximize diversity. Specifically, these datasets vary in the number of classes (2 to 1000), their target tasks, and domains. The benchmark encompasses a comprehensive range of tasks such as classification, scene understanding, geolocalization, object counting, and more, with the goal of rendering it extensively applicable across many applications. Further, the datasets span diverse domains, including natural, satellite, text, and medical images (See Tab. 3 for a comprehensive account of the datasets and their source). To ensure maximal compatibility, we have opted for tasks that permit the utilization of the same VLM architecture, precluding any requisite alterations or additional training. This approach necessitated the exclusion of tasks such as segmentation and object detection, which mandate additional training modules, introducing extraneous noise while evaluating VLM performance. However, it is worth noting that previous transferability works have shown that these approaches may generalize to more complex applications such as semantic segmentation [Pándy et al., 2022, Agostinelli et al., 2022].

A.2 LOVM Benchmark - Vision-Language Models

Tab. 4 presents a list of models and their corresponding pre-training datasets used in the LOVM benchmark. We utilize the open-clip library [Ilharco et al., 2021], a diverse collection of pre-trained VLMs spanning various architectures, including but not limited to CLIP and CoCa models, and utilizing encoders such as ResNet, ConvNext, and ViT. These models have undergone pre-training on various datasets, such as WIT [Radford et al., 2021], LAION 400m, and LAION 2b [Schuhmann et al., 2022], with different hyperparameters. From the 87 models currently available, we have carefully

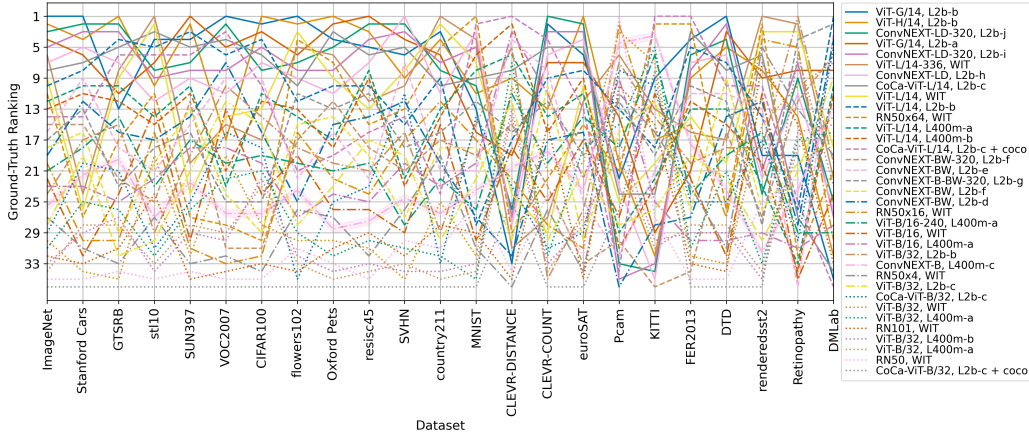


Figure 6: **Ground-Truth VLM Ranking.** As can be seen, there is a lot of variation in the ground-truth model ranking across both the natural image (left) and other (right) benchmarks.

selected 35 for our study. A comprehensive list of all models used in this benchmark can be found in Tab. 4. We avoided incorporating additional multi-modal models, such as BEIT[Wang et al., 2023] and VLMO [Bao et al., 2022], as these models utilize a shared text-image encoder and, therefore, cannot be evaluated on the same datasets as CoCa and CLIP. Using models from the open-clip library ensures maximum compatibility and reproducibility in our work. Currently, CLIP models comprise a significant portion of VLMs employed in practice. Tab. 4 includes 35 entries, each identified by an ID number. The first four columns indicate the ID number, model name, model abbreviation, and pre-training dataset name. The fifth column shows the abbreviation of the pre-training dataset name. The models listed in the table include ResNet (RN50, RN101, etc.) and Vision Transformer (ViT) with different sizes (B/32, B/16, L/14, etc.), and the pre-training datasets include OpenAI’s WIT dataset and two variants of LAION (L400m and L2b) datasets.

A.3 LOVM Benchmark - Ground-Truth Model Ranking

To evaluate the validity and generalizability of the LOVM benchmark, we first present the ground-truth model ranking over all datasets to show that the model order is not constant across the datasets. We organized the benchmarks from natural image classification (Fig. 6, left) to non-natural image / non-classification benchmarks (Fig. 6, right). As depicted in Fig. 6, the distribution exhibits a non-uniform pattern, indicating the utility of LOVM methods and the importance of VLM selection methods in general. Interestingly, ranking variations are more significant on the non-natural image / non-classification benchmarks. This exemplifies the need for LOVM methods to contend with content shift (i.e., changing what classes are in the target domain) and domain/task shift.

B Baseline Details

Fig. 7 shows an overview of our baselines. We first describe the prompting protocol used in Sec B.1. We then give an in-detail description of the scores used in the study in Sec. B.2. In Sec. B.3, we give additional details for the text dataset generation. Finally, in Sec. B.4, we describe how we use noise to corrupt the text caption dataset when calculating text-acc1 and text-f1 scores.

B.1 Prompting Templates

We use the same prompting strategy introduced by Radford et al. [2021] to generate the model zero-shot weights (see Fig. 10 for examples of templates from different datasets). Specifically, for every class c , we used the reported templates to produce the text prompts Y^c and encoded these prompts using the VLM text encoder, f_y , to produce the text embeddings for class c , \hat{y}^c :

$$\hat{y}^c = f_y(Y^c).$$

Table 3: Details on the different benchmarks used in the study, including the number of classes, tasks, and target domain.

Dataset	Classes	Task	Domain
Imagenet [Deng et al., 2009]	1000	classification	natural image
Stanford Cars [Krause et al., 2013]	196	classification	natural image
Flowers102 [Nilsback and Zisserman, 2008]	102	classification	natural image
CIFAR100 [Krizhevsky et al., 2009]	100	classification	natural image
GTSRB [Stallkamp et al., 2011]	43	classification	natural image
VOC2007 [Everingham et al., 2007]	20	classification	natural image
Oxford Pets [Parkhi et al., 2012]	37	classification	natural image
STL10 [Coates et al., 2011]	10	classification	natural image
DTD [Cimpoi et al., 2014]	46	classification	textural image
RESISC45 [Cheng et al., 2017]	45	classification	satellite images
EuroSAT [Helber et al., 2019]	10	classification	satellite images
MNIST [LeCun et al., 2010]	10	classification	hand-writing
Retinopathy [Kaggle and EyePacs, 2015]	5	classification	retina scan
PCam [Veeling et al., 2018]	2	classification	histopathology
SUN397 [Xiao et al., 2010]	397	scene und.	natural image
Country211 [Radford et al., 2021]	211	geolocation	natural image
SVHN [Netzer et al., 2011]	10	OCR	natural image
Rendered SST2 [Radford et al., 2021]	2	OCR	text image
FER2013 [Dumitru Ian Goodfellow, 2013]	7	fac. exp. rec.	natural image
CLEVR-C [Johnson et al., 2017]	8	object counting	natural image
CLEVR-D [Johnson et al., 2017]	8	distance est.	natural image
DMLab [Zhai et al., 2020]	6	distance est.	synthetic
KITTI [Geiger et al., 2013]	4	distance est.	natural image

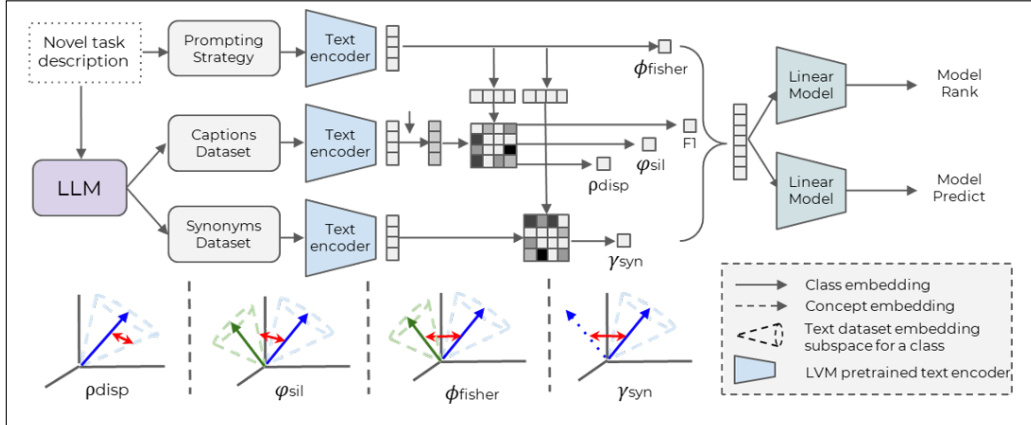


Figure 7: **Overview of the baselines.** (top left) Using a text description of a new task, we use a large language model to generate the Image Caption and Class-Synonym datasets. We feed these text datasets into a VLMs text encoder, which generates the text-derived multi-modal embeddings. Using these embeddings, as well as the user-defined prompting strategies, we extract different scores. Finally, we fit a linear model on the extracted scores to predict model ranking and accuracy. (bottom) Schematic drawings of our different proposed scores.

We then normalized each separate prompt by its L_2 norm and averaged the resulting vector to produce $\bar{\mathbf{y}}^c$, or the unnormalized zero-shot weight of class c :

$$\bar{\mathbf{y}}^c = \frac{1}{N} \sum_{j=1}^N \frac{\mathbf{y}_j^c}{\|\mathbf{y}_j^c\|_2},$$

where $\bar{\mathbf{y}}^c$ is then normalized again to produce the final zero-shot classification weight of class c ,

$$\mathbf{y}^c = \frac{\bar{\mathbf{y}}^c}{\|\bar{\mathbf{y}}^c\|_2}. \quad (4)$$

Table 4: **Translation of open clip to model/pre-training dataset names used in paper.** When renaming the datasets we tried to group models with similar optimization schemes to minimize the number of pre-training datasets without causing undo overlap.

ID	Model	Name	Dataset	Name
1	RN50	RN50	openai	WIT
2	RN101	RN101	openai	WIT
3	RN50x4	RN50x4	openai	WIT
4	RN50-16	RN50x16	openai	WIT
5	RN50x64	RN50x64	openai	WIT
6	ViT-B-32	ViT-B/32	laion400m_e31	L400m
7	ViT-B-32	ViT-B/32	laion400m_e32	L400m
8	ViT-B-32-quickgelu	ViT-B/32	laion400m_e32	L400m
9	ViT-B-32	ViT-B/32	openai	WIT
10	ViT-B-32	ViT-B/32	laion2b_s34b_b79k	L2b-b
11	ViT-B-32	ViT-B/32	laion2b_e16	L2b-c
12	ViT-B-16	ViT-B/16	laion400m_e32	L400m
13	ViT-B-16	ViT-B/16	openai	WIT
14	ViT-B-16-240	ViT-B/16-240	laion400m_e32	L400m
15	ViT-L-14	ViT-L/14	laion400m_e31	L400m
16	ViT-L-14	ViT-L/14	laion400m_e32	L400m
17	ViT-L-14	ViT-L/14	laion2b_s32b_b82k	L2b-b
18	ViT-L-14	ViT-L/14	openai	WIT
19	ViT-L-14-336	ViT-L/14-336	openai	WIT
20	ViT-G-14	ViT-G/14	laion2b_s12b_b42k	L2b-a
21	ViT-G-14	ViT-G/14	laion2b_s34b_b88k	L2b-a
22	ViT-H-14	ViT-H/14	laion2b_s32b_b79k	L2b-b
23	coca_ViT-B-32	CoCa-ViT-B/32	laion2b_s13b_b90k	L2b-c
24	coca_ViT-B-32	CoCa-ViT-B/32	mscoco_finetuned_laion2b_s13b_b90k	L2b-c + coco
25	coca_ViT-L-14	CoCa-ViT-L/14	laion2b_s13b_b90k	L2b-c
26	coca_ViT-L-14	CoCa-ViT-L/14	mscoco_finetuned_laion2b_s13b_b90k	L2b-c + coco
27	convnext_base	ConvNEXT-B	laion400m_s13b_b51k	L400m-c
28	convnext_base_w	ConvNEXT-BW	laion2b_s13b_b82k	L2b-d
29	convnext_base_w	ConvNEXT-BW	laion2b_s13b_b82k_augreg	L2b-e
30	convnext_base_w	ConvNEXT-BW	laion_aesthetic_s13b_b82k	L2b-f
31	convnext_base_w_320	ConvNEXT-BW-320	laion_aesthetic_s13b_b82k	L2b-f
32	convnext_base_w_320	ConvNEXT-BW-320	laion_aesthetic_s13b_b82k_augreg	L2b-g
33	convnext_large_d	ConvNEXT-LD	laion2b_s26b_b102k_augreg	L2b-h
34	convnext_large_d_320	ConvNEXT-LD-320	laion2b_s29b_b131k_ft	L2b-i
35	convnext_large_d_320	ConvNEXT-LD-320	laion2b_s29b_b131k_ft_soup	L2b-j

B.2 Text-Derived Scores

We define the six scores we derived for model selection and performance prediction. The *Text top-1 accuracy score* and *Text f1-score* is used to estimate the VLMs’ performance on a vision task using text as a proxy, while the *Fisher criterion* and *Silhouette score* are used to understand the VLM’s capability to separate samples from different classes in the target task (inter-class similarity). To estimate dataset granularity, we use *Class Dispersion score*. Finally, the *Synonym Consistency score* allows us to evaluate the degree of content shift between the VLMs’ pre-training and target dataset (intra-class similarity).

Text Classification scores. We use the generated captions dataset (see Sec. 3.1) as a proxy for images and evaluate the resulting model performance. Specifically, we use the VLM text encoder to generate text-derived multi-modal embeddings. We then corrupt these embeddings with Gaussian noise to approximate image-instance variation (see Sec. B.4) and calculate their cosine similarity with the class prompt embeddings - derived using the same prompt ensembling strategies proposed by Radford et al. [2021] (see Fig. 7). We then calculate the text top-1 accuracy (**text-acc1**) and text f1-score (**text-f1**).

Fisher criterion, ϕ_{fisher} . The Fisher criterion [Fisher, 1936] has been widely used as a dataset granularity measure and has recently been shown to be effective for classification by Cui et al. [2019]. The Fisher score measures the degree of similarity of the classes or the extent of their separation. In VLMs, The quality of the class separation can be evaluated using text by assessing how close the

different (text-derived) class prompt embeddings are. We introduce the concept of *Fisher criterion*, a score that quantifies how close the class prompt embeddings are to each other (see Fig. 7):

$$\phi_{\text{fisher}} = \frac{1}{C} \sum_{j=1}^C \max_{c, c \neq j} [\theta(\mathbf{y}^j, \mathbf{y}^c)], \quad (5)$$

where \mathbf{y}^c is the class prompt embedding derived using the prompt ensembling strategies proposed in Radford et al. [2021] for class c (see Sec. B.1), $\theta(\cdot, \cdot)$ is a function that calculates the cosine similarity between two vectors, and C is the number of classes.

Silhouette score, φ_{sil} . The silhouette score [Rousseeuw, 1987] is a well-established score that has been used to quantify the tightness of the same-class samples to the separation of different-class samples [Scheidegger et al., 2018, Cui et al., 2019]. Inspired by this score, we introduce the text-based *Silhouette score*, φ_{sil} , which measures the separation of different-class samples in the caption dataset D^{cap} . To do so, we evaluate the average cosine similarity of captions to the nearest other class by:

$$\varphi_{\text{sil}} = \frac{1}{C} \sum_{j=1}^C \max_{c, c \neq j} \left[\frac{1}{N} \sum_{k=1}^N \theta(D^{\text{cap}}[j]_k, \mathbf{y}^c) \right], \quad (6)$$

where \mathbf{y}^c is the class prompt embedding derived using the prompt ensembling strategies proposed in Radford et al. [2021] for class c (see Sec. B.1), $\theta(\cdot, \cdot)$ is a function that calculates the cosine similarity between two vectors, and C is the number of classes. $D^{\text{cap}}[j]_k$ representing sample k of class j in the caption dataset D^{cap} , and there is a total of N such samples in for each class.

Class Dispersion score, ρ_{disp} . The *Class Dispersion score* is used as the normalization constant to generate the Fisher and Silhouette scores, and it quantifies the degree of same-class tightness or data cone radius (see Fig. 7).

$$\rho_{\text{disp}} = \frac{1}{CN} \sum_{c=1}^C \sum_{k=1}^N \theta(D^{\text{cap}}[c]_k, \mathbf{y}^c), \quad (7)$$

where \mathbf{y}^c is the class prompt embedding derived using the prompt ensembling strategies proposed in Radford et al. [2021] for class c (see Sec. B.1), $\theta(\cdot, \cdot)$ is a function that calculates the cosine similarity between two vectors, and C is the number of classes. $D^{\text{cap}}[c]_k$ representing sample k of class c in the caption dataset D^{cap} , and there is a total of N such samples in for each class.

Synonym Consistency score, γ_{syn} . Synonym consistency has been shown in large language models to correlate with the degree of familiarity of the model with a particular concept [van der Lee et al., 2022]. Using the Synonym dataset, we compare the cosine similarity between the text embedding of each class and its corresponding synonyms. A high cosine similarity between the class and its corresponding synonyms/supercategories indicates that the model is aware of the semantic meaning of the class and is defined as:

$$\gamma_{\text{syn}} = \frac{1}{CN} \sum_{c=1}^C \sum_{k=1}^N \theta(D^{\text{syn}}[c]_k, \mathbf{y}^c), \quad (8)$$

where \mathbf{y}^c is the class prompt embedding derived using the prompt ensembling strategies proposed in Radford et al. [2021] for class c (see Sec. B.1), $\theta(\cdot, \cdot)$ is a function that calculates the cosine similarity between two vectors, and C is the number of classes. $D^{\text{syn}}[c]_k$ representing sample k of class c in the synonym dataset D^{syn} , and there is a total of N such samples in for each class.

B.3 Text Dataset Generation

To generate the Captions dataset, we used a large language model to generate realistic (but confusing) image captions. It was necessary to request confusing image captions to get sufficient variation in the image captions. We used OpenAI’s ‘gpt-3.5-turbo-0301’ model with a temperature of 1. For the synonym dataset, we reduced the temperature to 0.1 and only requested the synonyms themselves. We then used the prompting templates with the synonym in place of the original class name to generate D^{syn} .

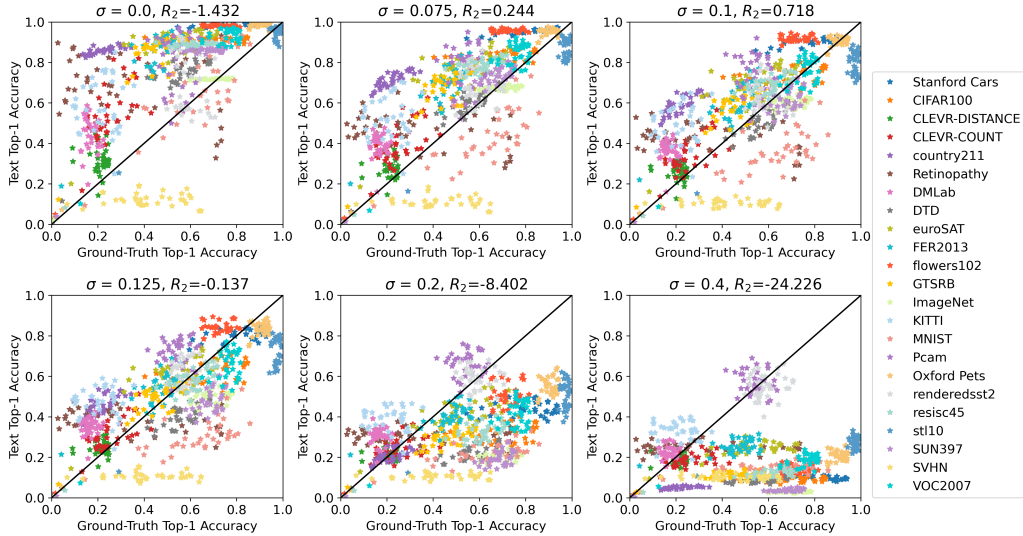


Figure 8: **Ablating Noise Injection Effect on Text Top-1 Accuracy.** Without noise ($\sigma=0$), the text top-1 accuracy saturates on many datasets and models, with extremely high top-1 accuracy, making the correlation between the ground-truth top-1 accuracy and text top-1 accuracy quite poor. By corrupting the text embeddings with noise, we notice an improvement in correlation up to $\sigma=0.1$, after which the correlation is steadily corrupted.

B.4 Text Classification and Noise Corruption

In this work, we introduce the use of Gaussian noise to corrupt text-derived multi-modal embeddings to approximate image-instance variation. The corrupted embeddings are then used to calculate the text top-1 accuracy and text-f1 score, which serves as a proxy for evaluating the performance of a vision model. The scores are derived from the Captions dataset, a collection of complex but probable image captions generated using a large language model for images containing the user-provided classes in the user-provided domain and for the user-provided task. For more, see Sec. 3.1.

To evaluate the effectiveness of the text top-1 accuracy, we systematically increase the level of noise corruption and plot the text top-1 accuracy against the ground-truth top-1 accuracy (See Fig. 8). We quantify this correlation via the R^2 score or the degree of explained variance. As we do not fit a linear model to the predicted vs. ground-truth predictions, R^2 ranges from 1 (perfect linear fit) to $-\infty$, where non of the variance is explained. The results show that, without noise corruption, the text top-1 accuracy is too high and frequently saturates without any corruption. However, as the noise level increases to 0.1, the text top-1 accuracy progressively improves until a better linear correlation can be seen. This indicates that increasing noise corruption can better approximate image-instance variation and improve the correlation of the text top-1 accuracy. Beyond 0.1, however, the correlation between the text top-1 accuracy and top-1 accuracy progressively worsens. This shows that while noise corruption helps improve the correlation of the text top-1 accuracy, there is a limit beyond which further noise corruption degrades its effectiveness.

C Additional Results

C.1 LOVM Per-Dataset Breakdown

Here, we show the per-dataset breakdown of our main results. In Tab. 5, we show our model ranking and performance prediction results for top-1 accuracy. In Tab. 6, we show our model ranking and performance prediction results for mean per-class recall.

Table 5: **LOVM Benchmark (top-1 accuracy)**. We evaluate our method’s performance over 23 datasets and 35 pre-trained models. (top) Model Ranking results. (bottom) Performance Prediction results. INB - ImageNet Benchmark score, C - Text Classification scores G - Granularity Scores.

		Stanford Cars	CIFAR100	CLEVR-DIST.	CLEVR-COUNT	Country211	Retinopathy	DMLab	DTD	EuroSAT	FER2013	Flowers102	GTSRB	ImageNet	KITTI	MNIST	PCam	Oxford Pets	Rendered SST2	RESISC45	STL10	SUN397	SVHN	VOC2007	Mean
R_5	INB	0.80	0.80	0.00	0.60	0.40	0.00	0.00	1.00	0.60	0.20	0.40	0.60	1.00	0.00	0.20	0.00	0.80	0.00	1.00	0.20	0.60	0.60	0.60	0.452
	C	0.00	0.20	0.20	0.60	0.40	0.00	0.00	0.60	0.40	0.40	0.20	0.40	0.00	0.20	0.20	0.20	0.00	0.20	0.40	0.20	0.40	0.00	0.00	0.226
	G	0.40	0.40	0.20	0.20	0.40	0.00	0.00	0.40	0.20	0.20	0.80	0.20	0.40	0.20	0.00	0.20	0.40	0.00	0.40	0.20	0.40	0.00	0.20	0.252
	G+C	0.40	0.40	0.20	0.20	0.40	0.00	0.00	0.40	0.20	0.20	0.80	0.20	0.40	0.20	0.00	0.20	0.40	0.00	0.40	0.20	0.40	0.00	0.20	0.252
	INB+C	0.80	0.80	0.00	0.60	0.60	0.00	0.00	1.00	0.60	0.20	0.60	0.60	0.80	0.00	0.20	0.20	0.80	0.00	1.00	0.20	0.60	0.40	0.60	0.461
	INB+G	0.80	0.80	0.00	0.60	0.40	0.00	0.00	1.00	0.60	0.20	0.40	0.60	1.00	0.00	0.40	0.00	0.80	0.20	1.00	0.40	0.60	0.40	0.40	0.461
INB+C+G	0.80	0.80	0.00	0.60	0.40	0.00	0.00	1.00	0.60	0.20	0.40	0.60	1.00	0.00	0.40	0.00	0.80	0.20	1.00	0.40	0.60	0.40	0.40	0.461	
τ	INB	0.33	0.67	0.00	0.33	0.00	0.00	0.00	-0.20	1.00	0.00	0.00	1.00	1.00	0.00	0.00	0.00	0.00	0.00	-0.40	0.00	-1.00	0.33	1.00	0.177
	C	0.00	0.00	0.00	1.00	0.00	0.00	0.00	0.33	0.00	0.00	0.00	0.00	0.00	0.00	0.00	0.00	0.00	0.00	0.00	0.00	0.00	0.00	0.00	0.058
	G	0.00	0.00	0.00	0.00	0.00	0.00	0.00	0.00	0.00	0.00	0.00	0.00	0.00	0.00	0.00	0.00	0.00	0.00	0.00	0.00	0.00	0.00	0.00	-0.014
	C+G	0.00	0.00	0.00	0.00	0.00	0.00	0.00	0.00	0.00	0.00	-0.33	0.00	0.00	0.00	0.00	0.00	0.00	0.00	0.00	0.00	0.00	0.00	0.00	-0.014
	INB+C	0.33	0.67	0.00	0.33	-0.33	0.00	0.00	0.00	1.00	0.00	1.00	1.00	1.00	0.00	0.00	0.00	0.33	0.00	-0.20	0.00	-1.00	0.00	1.00	0.223
	INB+G	0.33	0.33	0.00	0.33	0.00	0.00	0.00	0.00	1.00	0.00	0.00	1.00	1.00	0.80	0.00	0.00	0.00	0.00	-0.60	0.00	-1.00	0.00	0.00	0.096
INB+C+G	0.33	0.67	0.00	0.33	-0.33	0.00	0.00	0.00	1.00	0.00	1.00	1.00	1.00	0.00	0.00	0.00	0.33	0.00	-0.20	0.00	-1.00	0.00	1.00	0.223	
L_1	INB	0.16	0.07	0.58	0.42	0.49	0.52	0.61	0.09	0.08	0.26	0.01	0.26	0.00	0.50	0.03	0.26	0.17	0.18	0.06	0.21	0.03	0.17	0.08	0.228
	C	0.08	0.13	0.19	0.15	0.25	0.25	0.32	0.17	0.05	0.13	0.15	0.03	0.19	0.37	0.28	0.34	0.10	0.14	0.05	0.23	0.21	0.16	0.07	0.176
	G	0.03	0.03	0.19	0.22	0.44	0.16	0.23	0.01	0.03	0.07	0.45	0.01	0.22	0.29	0.29	0.04	0.09	0.11	0.02	0.21	0.03	0.10	0.02	0.143
	C+G	0.03	0.03	0.19	0.22	0.44	0.16	0.23	0.01	0.03	0.07	0.45	0.01	0.22	0.29	0.29	0.04	0.09	0.11	0.02	0.21	0.03	0.10	0.02	0.143
	INB+C	0.08	0.13	0.19	0.15	0.25	0.25	0.32	0.17	0.05	0.13	0.15	0.03	0.19	0.37	0.28	0.34	0.10	0.14	0.05	0.23	0.21	0.16	0.07	0.176
	INB+G	0.03	0.02	0.20	0.20	0.44	0.02	0.28	0.01	0.02	0.10	0.43	0.02	0.21	0.33	0.25	0.03	0.06	0.12	0.00	0.23	0.03	0.22	0.00	0.141
INB+C+G	0.03	0.02	0.20	0.20	0.44	0.02	0.28	0.01	0.02	0.10	0.43	0.02	0.21	0.33	0.25	0.03	0.06	0.12	0.00	0.23	0.03	0.22	0.00	0.141	

Table 6: **LOVM Benchmark (mean per-class recall)**. We evaluate our method’s performance over 23 datasets and 35 pre-trained models. (top) Model Ranking results. (bottom) Performance Prediction results. INB - ImageNet Benchmark score, C - Text Classification scores G - Granularity Scores.

		Stanford Cars	CIFAR100	CLEVR-DIST.	CLEVR-COUNT	Country211	Retinopathy	DMLab	DTD	EuroSAT	FER2013	Flowers102	GTSRB	ImageNet	KITTI	MNIST	PCam	Oxford Pets	Rendered SST2	RESISC45	STL10	SUN397	SVHN	VOC2007	Mean
R_5	INB	0.80	0.80	0.40	0.60	0.40	0.40	0.00	1.00	0.60	0.40	0.60	0.60	1.00	0.20	0.20	0.00	0.60	0.00	1.00	0.20	0.80	0.60	0.40	0.504
	C	0.00	0.20	0.20	0.60	0.40	0.20	0.20	0.60	0.40	0.40	0.00	0.40	0.00	0.40	0.20	0.20	0.20	0.20	0.40	0.20	0.40	0.00	0.00	0.252
	G	0.40	0.40	0.20	0.20	0.40	0.00	0.40	0.40	0.20	0.20	0.60	0.20	0.40	0.40	0.00	0.20	0.40	0.00	0.40	0.20	0.40	0.20	0.00	0.270
	G+C	0.00	0.40	0.20	0.20	0.60	0.40	0.60	0.40	0.20	0.20	0.00	0.60	0.20	0.20	0.40	0.20	0.00	0.00	0.40	0.20	0.40	0.20	0.00	0.261
	INB+C	0.80	0.80	0.40	0.60	0.60	0.40	0.00	1.00	0.60	0.40	0.80	0.60	0.80	0.20	0.20	0.20	0.80	0.00	1.00	0.20	0.80	0.40	0.40	0.522
	INB+G	0.80	0.80	0.40	0.60	0.40	0.40	0.00	1.00	0.60	0.40	0.60	0.60	1.00	0.20	0.40	0.20	0.60	0.00	1.00	0.40	0.80	0.60	0.60	0.539
INB+C+G	0.80	0.80	0.40	0.60	0.40	0.40	0.00	1.00	0.60	0.40	0.60	0.60	1.00	0.20	0.40	0.20	0.60	0.00	1.00	0.40	0.80	0.60	0.60	0.539	
τ	INB	0.67	0.67	0.00	0.33	0.00	0.00	0.00	0.00	1.00	0.00	1.00	1.00	1.00	0.00	0.00	0.00	-0.33	0.00	-0.40	0.00	-0.33	-0.33	0.00	0.186
	C	0.00	0.00	0.00	1.00	0.00	0.00	0.00	0.33	0.00	0.00	0.00	0.00	0.00	0.00	0.00	0.00	0.00	0.00	0.00	0.00	0.00	0.00	0.00	0.058
	G	0.00	0.00	0.00	0.00	0.00	0.00	0.00	0.00	0.00	0.00	-0.33	0.00	0.00	0.00	0.00	0.00	0.00	0.00	0.00	0.00	0.00	0.00	0.00	-0.014
	C+G	0.00	0.00	0.00	0.00	1.00	0.00	1.00	0.00	0.00	0.00	0.00	0.33	0.00	0.00	0.00	0.00	0.00	0.00	0.00	0.00	0.00	0.00	0.00	0.101
	INB+C	0.67	0.67	0.00	0.33	-0.33	0.00	0.00	-0.20	1.00	0.00	1.00	1.00	1.00	0.00	0.00	0.00	0.00	0.00	-0.20	0.00	0.00	0.00	0.00	0.214
	INB+G	0.67	0.33	0.00	0.33	0.00	0.00	0.00	0.00	1.00	0.00	1.00	1.00	0.80	0.00	0.00	0.00	0.33	0.00	-0.60	0.00	-0.33	-0.33	0.33	0.197
INB+C+G	0.67	0.33	0.00	0.33	0.00	0.00	0.00	0.00	1.00	0.00	1.00	1.00	0.80	0.00	0.00	0.00	0.33	0.00	-0.60	0.00	-0.33	-0.33	0.33	0.197	
L_1	INB	0.16	0.07	0.58	0.42	0.49	0.52	0.61	0.09	0.08	0.26	0.01	0.26	0.00	0.50	0.03	0.26	0.17	0.18	0.06	0.21	0.03	0.17	0.08	0.228
	C	0.07	0.09	0.22	0.14	0.26	0.27	0.31	0.16	0.03	0.15	0.17	0.08	0.22	0.33	0.30	0.34	0.09	0.16	0.05	0.22	0.20	0.21	0.12	0.183
	G	0.14	0.03	0.25	0.16	0.44	0.23	0.19	0.01	0.01	0.12	0.46	0.03	0.30	0.15	0.28	0.03	0.07	0.09	0.04	0.17	0.02	0.09	0.02	0.145
	C+G	0.14	0.03	0.25	0.16	0.44	0.23	0.19	0.01	0.01	0.12	0.46	0.03	0.30	0.15	0.28	0.03	0.07	0.09	0.04	0.17	0.02	0.09	0.02	0.145
	INB+C	0.07	0.09	0.22	0.14	0.26	0.27	0.31	0.16	0.03	0.15	0.17	0.08	0.22	0.33	0.30	0.34	0.09	0.16	0.05	0.22	0.20	0.21	0.12	0.183
	INB+G	0.14	0.03	0.25	0.16	0.44	0.23	0.19	0.01	0.01	0.12	0.46	0.03	0.30	0.15	0.28	0.03	0.07	0.09	0.04	0.17	0.02	0.09	0.02	0.145
INB+C+G	0.14	0.03	0.25	0.16	0.44	0.23	0.19	0.01	0.01	0.12	0.46	0.03	0.30	0.15	0.28	0.03	0.07	0.09	0.04	0.17	0.02	0.09	0.02	0.145	

C.2 Ablation Experiments

To understand the utility of each of our extracted scores, we exhaustively ablated their effect on top-1 accuracy model ranking and performance prediction (Tab. 7 and Tab. 8), and mean per-class recall model ranking and performance prediction (Tab. 9 and Tab. 10). Specifically, we ablated each score’s impact on the resulting model’s performance. As can be seen, using more than ~ 3 features at a time seldom improves performance. Future work can investigate the use of more sophisticated models that may be able to utilize more scores in predicting model ranking and performance. Specifically, for ranking models, text classification and scores quantifying intra-class similarity (Class Dispersion score & Synonym Consistency score) were the most dominant, while for performance prediction, granularity scores quantifying both inter- and intra-class similarity was the most important. This

Table 7: **LOVM Model Selection Ablation.** Here, we ablate all the different scores used in our baselines for model ranking by top-1 accuracy. We separated the text classification (C) base scores, and the granularity-based scores that quantify inter- and intra-class similarity. a_{IN} - Imagenet Accuracy, ϕ_{fisher} - Fisher criterion, text-f1 - caption dataset f1-score, text-acc1 - text top-1 accuracy, γ_{syn} - Synonym Consistency score, φ_{sil} - Silhouette score, ρ_{disp} - Class Dispersion score.

	Scores								Metrics			Scores								Metrics	
	Row ID	a_{IN}	text-f1	text-acc1	γ_{syn}	ρ_{disp}	φ_{sil}	ϕ_{fisher}	τ (\uparrow)	R_5 (\uparrow)		Row ID	a_{IN}	text-f1	text-acc1	γ_{syn}	ρ_{disp}	φ_{sil}	ϕ_{fisher}	τ (\uparrow)	R_5 (\uparrow)
Model Ranking	1	✓	×	×	×	×	×	0.177	0.452	65	✓	✓	✓	×	✓	×	×	0.107	0.443		
	2	×	✓	×	×	×	×	0.058	0.226	66	✓	✓	✓	×	×	×	×	0.093	0.435		
	3	×	×	✓	×	×	×	0.029	0.191	67	✓	✓	✓	×	×	×	×	0.133	0.443		
	4	×	×	×	✓	×	×	0.000	0.183	68	✓	✓	×	×	×	×	×	0.174	0.443		
	5	×	×	×	×	✓	×	-0.014	0.243	69	✓	✓	×	✓	×	×	×	0.157	0.443		
	6	×	×	×	×	×	✓	×	-0.014	0.252	70	✓	✓	×	✓	×	×	×	0.075	0.417	
	7	×	×	×	×	×	×	✓	0.000	0.165	71	✓	✓	×	×	×	×	×	0.113	0.452	
	8	✓	✓	×	×	×	×	×	0.223	0.461	72	✓	✓	×	×	✓	×	×	0.096	0.417	
	9	✓	×	✓	×	×	×	×	0.200	0.452	73	✓	×	×	×	×	×	✓	0.096	0.417	
	10	✓	×	×	✓	×	×	×	0.188	0.426	74	✓	×	×	×	×	×	×	0.159	0.435	
	11	✓	×	×	×	✓	×	×	0.096	0.461	75	✓	×	✓	✓	×	×	×	0.128	0.443	
	12	✓	×	×	×	×	✓	×	0.078	0.417	76	✓	×	✓	✓	×	×	×	0.075	0.417	
	13	✓	×	×	×	×	×	✓	0.119	0.426	77	✓	×	✓	×	×	×	×	0.113	0.452	
	14	×	✓	✓	×	×	×	×	0.029	0.226	78	✓	×	✓	×	✓	×	×	0.096	0.417	
	15	×	✓	×	×	✓	×	×	0.043	0.191	79	✓	×	×	×	✓	×	✓	0.096	0.417	
	16	×	✓	×	×	×	✓	×	0.014	0.209	80	✓	×	×	×	×	✓	✓	0.043	0.417	
	17	×	✓	×	×	×	×	✓	0.014	0.217	81	✓	×	×	×	×	✓	✓	0.119	0.417	
	18	×	✓	×	×	×	×	✓	0.000	0.183	82	✓	×	×	×	✓	✓	✓	0.119	0.417	
	19	×	×	✓	×	✓	×	×	0.043	0.191	83	✓	×	×	×	×	✓	✓	0.110	0.417	
	20	×	×	✓	×	×	✓	×	0.014	0.209	84	×	✓	✓	×	×	×	×	-0.029	0.209	
	21	×	×	×	✓	×	×	✓	0.014	0.191	85	×	✓	✓	✓	×	×	×	-0.029	0.217	
	22	×	×	×	✓	×	×	✓	0.000	0.174	86	×	✓	✓	×	×	×	✓	-0.014	0.217	
	23	×	×	×	✓	×	×	×	0.000	0.200	87	×	✓	✓	×	×	×	×	0.014	0.200	
	24	×	×	×	✓	×	✓	×	0.014	0.235	88	×	✓	✓	×	×	×	✓	0.014	0.226	
	25	×	×	×	✓	×	×	✓	0.000	0.174	89	×	✓	✓	×	×	×	✓	0.014	0.217	
	26	×	×	×	✓	×	✓	×	0.014	0.209	90	×	✓	×	✓	×	×	×	0.014	0.217	
	27	×	×	×	×	×	×	✓	0.000	0.165	91	×	✓	×	✓	×	×	✓	0.000	0.226	
	28	✓	×	✓	×	×	×	✓	0.014	0.200	92	×	✓	×	×	×	✓	✓	0.014	0.209	
	29	✓	×	✓	×	×	×	×	0.093	0.443	93	×	✓	×	×	×	✓	✓	0.014	0.209	
	30	✓	✓	×	×	×	×	×	0.174	0.443	94	×	×	×	✓	✓	✓	×	0.014	0.209	
	31	✓	✓	×	×	×	×	×	0.188	0.435	95	×	×	✓	✓	✓	×	×	0.014	0.217	
	32	✓	✓	×	×	×	×	×	0.145	0.443	96	×	×	✓	×	×	×	✓	0.014	0.209	
	33	✓	✓	×	×	×	×	✓	0.096	0.417	97	×	×	✓	×	×	✓	✓	0.014	0.200	
	34	✓	×	✓	×	×	×	×	0.159	0.435	98	×	×	×	✓	✓	✓	✓	0.014	0.226	
	35	✓	×	✓	×	×	×	×	0.188	0.443	99	×	×	×	✓	✓	×	×	0.116	0.435	
	36	✓	×	✓	×	×	✓	×	0.145	0.452	100	✓	✓	✓	✓	×	×	×	0.058	0.435	
	37	✓	×	✓	×	×	×	✓	0.067	0.417	101	✓	✓	✓	✓	×	×	×	0.133	0.443	
	38	✓	×	×	×	✓	✓	×	0.110	0.426	102	✓	✓	✓	×	×	×	×	0.049	0.443	
	39	✓	×	×	×	✓	×	✓	0.188	0.426	103	✓	✓	✓	×	×	×	✓	0.133	0.443	
	40	✓	×	×	×	✓	×	×	0.119	0.417	104	✓	✓	✓	×	×	✓	✓	0.133	0.443	
	41	✓	×	×	×	×	✓	✓	0.067	0.435	105	✓	✓	×	×	×	✓	×	0.128	0.443	
	42	✓	×	×	×	×	✓	×	0.119	0.417	106	✓	✓	×	✓	×	✓	×	0.104	0.417	
	43	✓	×	×	×	×	×	✓	0.119	0.426	107	✓	✓	×	×	×	✓	✓	0.104	0.417	
	44	×	✓	✓	✓	×	×	×	0.000	0.209	108	✓	✓	×	×	×	×	✓	0.128	0.435	
	45	×	✓	✓	✓	×	×	×	0.014	0.200	109	✓	×	✓	✓	✓	×	×	0.128	0.443	
	46	×	✓	✓	✓	×	×	✓	0.014	0.209	110	✓	×	✓	✓	✓	×	×	0.104	0.417	
	47	×	✓	✓	✓	×	×	✓	0.014	0.209	111	✓	×	✓	×	×	✓	✓	0.104	0.417	
	48	×	✓	×	×	✓	×	×	0.000	0.217	112	✓	×	✓	×	×	✓	✓	0.128	0.435	
	49	×	✓	×	×	✓	×	✓	0.014	0.217	113	✓	×	×	✓	✓	✓	✓	0.101	0.400	
	50	×	✓	×	×	×	×	×	0.000	0.191	114	×	×	×	✓	✓	×	×	-0.029	0.217	
	51	×	✓	×	×	×	✓	✓	0.014	0.209	115	×	✓	✓	×	×	×	✓	-0.043	0.209	
	52	×	✓	×	×	×	×	✓	0.014	0.217	116	×	✓	✓	×	×	×	✓	-0.029	0.217	
	53	×	✓	×	×	×	×	✓	0.014	0.209	117	×	✓	✓	×	×	✓	✓	0.014	0.217	
	54	×	×	×	✓	×	×	×	0.014	0.217	118	×	✓	×	×	✓	✓	✓	0.014	0.209	
	55	×	×	×	✓	×	✓	×	0.014	0.209	119	×	×	×	✓	✓	✓	✓	0.014	0.209	
	56	×	×	×	✓	×	×	×	0.043	0.191	120	×	×	✓	✓	✓	✓	×	0.055	0.443	
	57	×	×	×	✓	×	×	✓	0.014	0.191	121	✓	✓	✓	✓	✓	×	✓	0.090	0.435	
	58	×	×	×	✓	×	×	✓	0.014	0.200	122	✓	✓	✓	✓	×	×	✓	0.090	0.435	
	59	×	×	×	✓	×	×	✓	0.014	0.200	123	✓	✓	✓	×	×	✓	✓	0.090	0.443	
	60	×	×	×	✓	✓	✓	×	0.014	0.200	124	✓	✓	×	×	✓	✓	✓	0.128	0.435	
	61	×	×	×	✓	×	×	✓	0.000	0.165	125	✓	×	×	✓	✓	✓	✓	0.128	0.435	
	62	×	×	×	✓	×	✓	✓	0.014	0.191	126	×	×	✓	✓	✓	✓	✓	-0.029	0.217	
	63	×	×	×	✓	×	✓	✓	0.014	0.191	127	✓	✓	✓	✓	✓	✓	✓	0.046	0.435	
	64	✓	✓	✓	✓	✓	×	×	0.151	0.452											

We ablate the model ranking performance to understand each extracted score’s effect on ranking models. The text classification scores and scores quantifying intra-class similarity were the most consequential in predicting model ranking. Specifically, in ranking models, the text-f1 score, Class Dispersion score (ρ_{disp}), and Synonym Consistency score (γ_{syn}) were the most dominant (Tab. 7 rows 8 & 11, Tab. 9 row 38). Overall, it seems like the text classification excelled at fine-grained ranking (as quantified by τ), while the inter-class granularity scores improved the coarse ranking prediction (as quantified by R_5). Meanwhile, granularity scores quantifying inter- and intra-class similarity were the most dominant for performance prediction. Specifically, Class Dispersion score (ρ_{disp}), Synonym Consistency score (γ_{syn}), and Silhouette score (φ_{sil}) were the most influential (Tab. 8 rows 26 & 41, Tab. 10 row 60). INB does not aid performance prediction, indicating that getting a course estimation of dataset difficulty dominates performance prediction.

Table 8: **LOVM Model Prediction Ablation.** Here, we ablate all the different scores used in our baselines for predicting model top-1 accuracy. We separated the text classification (C) base scores, and the granularity-based scores that quantify inter- and intra-class similarity. a_{IN} - Imagenet Accuracy, ϕ_{fisher} - Fisher criterion, text-f1 - caption dataset f1-score, text-acc1 - text top-1 accuracy, γ_{syn} - Synonym Consistency score, φ_{sil} - Silhouette score, ρ_{disp} - Class Dispersion score.

	Scores								Metrics
	Row ID	a_{IN}	text-f1	text-acc1	γ_{syn}	ρ_{disp}	φ_{sil}	ϕ_{fisher}	$L_1 (\downarrow)$
	1	✓	×	×	×	×	×	×	0.220
	2	×	✓	×	×	×	×	×	0.176
	3	×	×	✓	×	×	×	×	0.177
	4	×	×	×	✓	×	×	×	0.188
	5	×	×	×	×	✓	×	×	0.200
	6	×	×	×	×	×	✓	×	0.223
	7	×	×	×	×	×	×	✓	0.170
	8	✓	✓	×	×	×	×	×	0.189
	9	✓	×	✓	×	×	×	×	0.184
	10	✓	×	×	✓	×	×	×	0.215
	11	✓	×	×	×	✓	×	×	0.205
	12	✓	×	×	×	×	✓	×	0.215
	13	✓	×	×	×	×	×	✓	0.167
	14	×	✓	✓	×	×	×	×	0.180
	15	×	✓	×	✓	×	×	×	0.190
	16	×	✓	×	×	✓	×	×	0.184
	17	×	✓	×	×	×	✓	×	0.180
	18	×	✓	×	×	×	×	✓	0.160
	19	×	×	✓	✓	×	×	×	0.183
	20	×	×	✓	×	✓	×	×	0.176
	21	×	×	✓	×	×	✓	×	0.179
	22	×	×	✓	×	×	×	✓	0.159
	23	×	×	×	✓	✓	×	×	0.199
	24	×	×	×	✓	×	✓	×	0.188
	25	×	×	×	✓	×	×	✓	0.154
	26	×	×	×	×	✓	✓	×	0.143
	27	×	×	×	×	✓	×	✓	0.163
	28	×	×	×	×	✓	✓	×	0.166
	29	✓	✓	✓	×	×	×	×	0.191
	30	✓	✓	✓	×	×	×	×	0.197
	31	✓	✓	×	×	×	×	×	0.189
	32	✓	✓	×	×	✓	×	×	0.187
	33	✓	✓	×	×	×	×	✓	0.159
	34	✓	×	✓	✓	×	×	×	0.196
	35	✓	×	✓	×	✓	×	×	0.189
	36	✓	×	✓	×	×	✓	×	0.185
	37	✓	×	✓	×	×	×	✓	0.155
	38	✓	×	×	✓	✓	×	×	0.212
	39	✓	×	×	✓	×	✓	×	0.219
	40	✓	×	×	×	×	×	✓	0.156
	41	✓	×	×	×	✓	✓	×	0.141
	42	✓	×	×	×	✓	×	✓	0.160
	43	✓	×	×	×	×	✓	✓	0.167
	44	×	✓	✓	✓	×	×	×	0.184
	45	×	✓	✓	×	✓	×	×	0.187
	46	×	✓	✓	×	×	✓	×	0.186
	47	×	✓	✓	×	×	×	✓	0.170
	48	×	✓	×	✓	✓	×	×	0.190
	49	×	✓	×	✓	×	✓	×	0.189
	50	×	✓	×	×	×	×	✓	0.160
	51	×	✓	×	×	✓	✓	×	0.148
	52	×	✓	×	×	×	×	✓	0.163
	53	×	✓	×	×	×	✓	✓	0.167
	54	×	×	✓	✓	×	×	×	0.183
	55	×	×	✓	✓	×	✓	×	0.187
	56	×	×	✓	✓	×	×	✓	0.159
	57	×	×	✓	×	✓	×	×	0.147
	58	×	×	✓	×	✓	×	✓	0.159
	59	×	×	✓	×	×	✓	✓	0.167
	60	×	×	×	✓	✓	×	×	0.148
	61	×	×	×	✓	×	×	✓	0.154
	62	×	×	×	✓	×	✓	✓	0.161
	63	×	×	×	✓	×	✓	✓	0.153
	64	✓	×	✓	×	×	×	×	0.200

	Scores								Metrics
	Row ID	a_{IN}	text-f1	text-acc1	γ_{syn}	ρ_{disp}	φ_{sil}	ϕ_{fisher}	$L_1 (\downarrow)$
	65	✓	✓	✓	×	✓	×	×	0.191
	66	✓	✓	✓	×	×	✓	×	0.191
	67	✓	✓	✓	×	×	×	✓	0.167
	68	✓	✓	×	✓	✓	×	×	0.198
	69	✓	✓	×	✓	×	×	×	0.200
	70	✓	✓	×	✓	×	×	✓	0.160
	71	✓	✓	×	×	×	×	×	0.151
	72	✓	✓	×	×	✓	×	✓	0.158
	73	✓	✓	×	×	×	✓	✓	0.163
	74	✓	×	✓	×	✓	×	×	0.198
	75	✓	×	✓	✓	×	×	×	0.198
	76	✓	×	✓	✓	×	×	✓	0.158
	77	✓	×	✓	×	×	✓	×	0.156
	78	✓	×	✓	×	✓	×	✓	0.154
	79	✓	×	✓	×	×	✓	✓	0.162
	80	✓	×	×	✓	✓	✓	×	0.144
	81	✓	×	×	✓	✓	×	✓	0.158
	82	✓	×	×	✓	×	×	✓	0.164
	83	✓	×	×	×	✓	✓	✓	0.149
	84	×	✓	✓	✓	✓	×	×	0.186
	85	×	✓	✓	✓	×	×	×	0.194
	86	×	✓	✓	✓	×	×	✓	0.168
	87	×	✓	✓	×	×	×	×	0.152
	88	×	✓	✓	×	✓	×	✓	0.171
	89	×	✓	✓	×	×	✓	✓	0.177
	90	×	✓	×	✓	✓	×	×	0.156
	91	×	✓	×	✓	✓	×	✓	0.168
	92	×	✓	×	✓	×	×	✓	0.173
	93	×	✓	×	×	×	✓	✓	0.155
	94	×	×	✓	✓	✓	×	×	0.156
	95	×	×	✓	✓	✓	×	✓	0.166
	96	×	×	✓	✓	×	✓	✓	0.168
	97	×	×	✓	×	✓	✓	✓	0.158
	98	×	×	×	✓	✓	✓	✓	0.150
	99	✓	✓	✓	✓	✓	×	×	0.202
	100	✓	✓	✓	✓	×	×	×	0.198
	101	✓	✓	✓	✓	×	×	✓	0.164
	102	✓	✓	✓	×	✓	×	×	0.154
	103	✓	✓	✓	×	×	×	✓	0.164
	104	✓	✓	✓	×	×	✓	✓	0.165
	105	✓	✓	×	✓	✓	×	×	0.161
	106	✓	✓	×	✓	✓	×	✓	0.165
	107	✓	✓	×	✓	×	✓	✓	0.171
	108	✓	✓	×	×	✓	✓	✓	0.165
	109	✓	×	✓	✓	✓	×	×	0.159
	110	✓	×	✓	✓	✓	×	✓	0.165
	111	✓	×	✓	✓	×	×	✓	0.168
	112	✓	×	✓	×	✓	✓	✓	0.166
	113	✓	×	×	✓	✓	✓	✓	0.153
	114	×	✓	✓	✓	✓	×	×	0.162
	115	×	✓	✓	✓	✓	×	✓	0.175
	116	×	✓	✓	✓	×	✓	✓	0.178
	117	×	✓	✓	×	✓	✓	✓	0.159
	118	×	✓	×	✓	✓	✓	✓	0.163
	119	×	×	✓	✓	✓	✓	✓	0.161
	120	✓	✓	✓	✓	✓	×	×	0.161
	121	✓	✓	✓	✓	✓	×	✓	0.171
	122	✓	✓	✓	✓	×	✓	✓	0.173
	123	✓	✓	✓	×	✓	✓	✓	0.162
	124	✓	✓	×	✓	✓	✓	✓	0.167
	125	✓	×	✓	✓	✓	✓	✓	0.164
	126	×	✓	✓	✓	✓	✓	✓	0.165
	127	✓	✓	✓	✓	✓	✓	✓	0.171

Table 9: **LOVM Model Selection Ablation.** Here, we ablate all the different scores used in our baselines for model ranking by mean per-class recall. We separated the text classification (C) base scores, and the granularity-based scores that quantify inter- and intra-class similarity. a_{IN} - Imagenet Accuracy, ϕ_{fisher} - Fisher criterion, text-f1 - caption dataset f1-score, text-acc1 - text top-1 accuracy, γ_{syn} - Synonym Consistency score, φ_{sil} - Silhouette score, ρ_{disp} - Class Dispersion score.

	Scores									Metrics		
	Row ID	a_{IN}	text-f1	text-acc1	γ_{syn}	ρ_{disp}	φ_{sil}	ϕ_{fisher}	τ (\uparrow)	R_5 (\uparrow)		
Model Ranking	1	✓	×	×	×	×	×	×	0.186	0.504		
	2	×	✓	×	×	×	×	×	0.058	0.252		
	3	×	×	✓	×	×	×	×	0.029	0.191		
	4	×	×	×	✓	×	×	×	-0.014	0.217		
	5	×	×	×	×	✓	×	×	0.014	0.261		
	6	×	×	×	×	×	✓	×	-0.014	0.270		
	7	×	×	×	×	×	×	✓	0.000	0.157		
	8	✓	✓	×	×	×	×	×	0.214	0.522		
	9	✓	×	✓	×	×	×	×	0.209	0.513		
	10	✓	×	×	✓	×	×	×	0.116	0.487		
	11	✓	×	×	×	✓	×	×	0.177	0.530		
	12	✓	×	×	×	×	✓	×	0.186	0.504		
	13	✓	×	×	×	×	×	✓	0.072	0.478		
	14	×	✓	✓	×	×	×	×	0.029	0.235		
	15	×	✓	×	✓	×	×	×	0.072	0.235		
	16	×	✓	×	×	✓	×	×	0.014	0.243		
	17	×	✓	×	×	×	✓	×	0.014	0.252		
	18	×	✓	×	×	×	×	✓	0.014	0.235		
	19	×	×	✓	×	×	×	×	0.072	0.252		
	20	×	×	✓	×	✓	×	×	0.043	0.243		
	21	×	×	✓	×	×	✓	×	0.043	0.226		
	22	×	×	✓	×	×	×	✓	0.043	0.226		
	23	×	×	×	✓	×	×	×	-0.014	0.217		
	24	×	×	×	✓	×	✓	×	0.000	0.252		
	25	×	×	×	✓	×	×	✓	0.000	0.174		
	26	×	×	×	×	✓	×	✓	0.000	0.226		
	27	×	×	×	×	✓	×	✓	0.000	0.165		
	28	×	×	×	×	×	✓	✓	0.000	0.217		
	29	✓	✓	✓	×	×	×	×	0.145	0.487		
	30	✓	✓	×	✓	×	×	×	0.214	0.504		
	31	✓	✓	×	×	✓	×	×	0.200	0.504		
	32	✓	✓	×	×	×	✓	×	0.180	0.496		
	33	✓	✓	×	×	×	×	✓	0.122	0.496		
	34	✓	×	✓	✓	×	×	×	0.194	0.496		
	35	✓	×	✓	×	✓	×	×	0.180	0.504		
	36	✓	×	✓	×	×	✓	×	0.180	0.504		
	37	✓	×	✓	×	×	×	✓	0.136	0.504		
	38	✓	×	×	✓	×	×	×	0.197	0.539		
	39	✓	×	×	✓	×	✓	×	0.145	0.496		
	40	✓	×	×	×	×	✓	×	0.072	0.470		
	41	✓	×	×	×	✓	✓	×	0.174	0.487		
	42	✓	×	×	×	×	✓	✓	0.058	0.487		
	43	✓	×	×	×	×	✓	✓	0.072	0.487		
	44	×	✓	✓	✓	×	×	×	0.000	0.243		
	45	×	✓	✓	×	✓	×	×	0.043	0.235		
	46	×	✓	✓	×	×	✓	×	0.043	0.243		
	47	×	✓	✓	×	×	×	✓	0.000	0.226		
	48	×	✓	×	✓	✓	×	×	0.029	0.252		
	49	×	✓	×	✓	×	✓	×	0.043	0.243		
	50	×	✓	×	✓	×	×	✓	0.101	0.252		
	51	×	✓	×	×	✓	✓	×	0.043	0.252		
	52	×	✓	×	×	×	×	✓	0.043	0.243		
	53	×	✓	×	×	×	✓	✓	0.043	0.243		
	54	×	×	✓	✓	×	×	×	0.043	0.243		
	55	×	×	✓	✓	×	✓	×	0.043	0.252		
	56	×	×	✓	✓	×	×	×	0.101	0.261		
	57	×	×	✓	×	✓	✓	×	0.043	0.226		
	58	×	×	✓	×	×	✓	×	0.000	0.226		
	59	×	×	✓	×	×	✓	×	0.000	0.217		
	60	×	×	×	✓	✓	✓	×	0.000	0.226		
	61	×	×	×	✓	✓	×	✓	0.000	0.165		
	62	×	×	×	✓	✓	✓	✓	0.000	0.209		
	63	×	×	×	×	✓	✓	✓	0.014	0.226		
	64	✓	✓	✓	✓	×	×	×	0.130	0.478		

	Scores									Metrics		
	Row ID	a_{IN}	text-f1	text-acc1	γ_{syn}	ρ_{disp}	φ_{sil}	ϕ_{fisher}	τ (\uparrow)	R_5 (\uparrow)		
65	✓	✓	✓	×	✓	×	×	×	0.130	0.487		
66	✓	✓	✓	×	✓	×	×	×	0.130	0.478		
67	✓	✓	✓	×	×	×	×	×	0.145	0.478		
68	✓	✓	×	✓	×	×	×	×	0.194	0.496		
69	✓	✓	×	✓	×	✓	×	×	0.186	0.504		
70	✓	✓	×	✓	×	×	×	×	0.136	0.496		
71	✓	✓	×	×	×	✓	×	×	0.171	0.504		
72	✓	✓	×	×	×	✓	×	×	0.122	0.496		
73	✓	✓	×	×	×	✓	×	×	0.122	0.496		
74	✓	×	×	×	×	✓	×	×	0.194	0.496		
75	✓	×	✓	✓	×	✓	×	×	0.180	0.496		
76	✓	×	✓	✓	×	×	×	×	0.151	0.504		
77	✓	×	✓	×	×	×	×	×	0.171	0.513		
78	✓	×	✓	×	×	✓	×	×	0.151	0.504		
79	✓	×	✓	×	×	×	✓	✓	0.151	0.504		
80	✓	×	×	×	×	×	✓	×	0.130	0.487		
81	✓	×	×	×	×	×	✓	×	0.058	0.478		
82	✓	×	×	×	✓	×	✓	✓	0.058	0.478		
83	✓	×	×	×	×	✓	✓	✓	0.087	0.487		
84	×	×	×	×	×	✓	✓	×	0.000	0.235		
85	×	✓	✓	✓	×	✓	×	×	0.000	0.252		
86	×	✓	✓	✓	×	✓	×	×	0.043	0.261		
87	×	✓	✓	×	×	×	×	×	0.014	0.243		
88	×	✓	✓	×	×	×	×	×	0.043	0.235		
89	×	✓	✓	×	×	×	×	✓	0.043	0.235		
90	×	✓	×	×	×	✓	✓	×	0.043	0.243		
91	×	✓	×	×	✓	✓	×	×	0.029	0.261		
92	×	✓	×	×	×	×	✓	✓	0.043	0.243		
93	×	✓	×	×	×	✓	✓	✓	0.014	0.243		
94	×	×	×	✓	✓	✓	×	×	0.043	0.252		
95	×	×	×	✓	✓	✓	×	×	0.043	0.252		
96	×	×	×	×	×	✓	✓	✓	0.043	0.252		
97	×	×	×	×	×	✓	✓	✓	0.043	0.226		
98	×	×	×	×	×	✓	✓	✓	0.014	0.261		
99	×	×	×	×	×	✓	✓	×	0.130	0.487		
100	✓	✓	✓	✓	✓	×	×	×	0.116	0.487		
101	✓	✓	✓	✓	×	×	×	×	0.145	0.487		
102	✓	✓	✓	×	×	×	×	×	0.130	0.478		
103	✓	✓	✓	×	×	×	×	×	0.130	0.487		
104	✓	✓	✓	×	×	×	×	✓	0.130	0.487		
105	✓	✓	×	×	×	×	×	×	0.180	0.496		
106	✓	✓	×	×	×	×	×	×	0.136	0.496		
107	✓	✓	×	×	×	×	✓	✓	0.136	0.496		
108	✓	✓	×	×	×	×	✓	✓	0.136	0.496		
109	✓	×	×	×	×	×	✓	×	0.186	0.504		
110	✓	×	×	×	×	×	×	×	0.151	0.504		
111	✓	×	×	×	×	×	✓	✓	0.151	0.504		
112	✓	×	×	×	×	×	✓	✓	0.136	0.496		
113	✓	×	×	×	×	×	✓	✓	0.087	0.487		
114	×	×	×	×	×	×	×	×	0.000	0.252		
115	×	✓	✓	✓	✓	×	✓	✓	0.000	0.235		
116	×	✓	✓	✓	×	×	✓	✓	0.029	0.252		
117	×	✓	✓	×	×	×	✓	✓	0.014	0.235		
118	×	✓	×	×	×	×	✓	✓	0.043	0.252		
119	×	×	✓	✓	✓	✓	✓	✓	0.043	0.261		
120	✓	✓	✓	✓	✓	✓	✓	×	0.130	0.487		
121	✓	✓	✓	✓	✓	×	×	×	0.130	0.487		
122	✓	✓	✓	✓	×	×	✓	✓	0.130	0.487		
123	✓	✓	✓	×	×	✓	✓	✓	0.116	0.496		
124	✓	✓	×	×	✓	✓	✓	✓	0.136	0.496		
125	×	×	✓	✓	✓	✓	✓	✓	0.136	0.496		
126	×	×	✓	✓	✓	✓	✓	✓	0.043	0.252		
127	✓	✓	✓	✓	✓	✓	✓	✓	0.130	0.478		

C.3 Raw Model Ranking Details

To illustrate the model ranking of the naive (ImageNet Benchmark) baseline to some text-based approaches, we visualize the raw ranking prediction of each method. We sort the datasets from natural image classification (Fig. 9 left) to non-natural image / non-classification benchmarks (Fig. 9 right). Here, the evident failure of the ImageNet Benchmark baseline to capture dataset-specific changes in ranking is apparent. As the benchmark approach ranks models by their ImageNet performance, the model ranking is constant for all datasets. Meanwhile, integrating the text features produces a ranking distribution with a discernible positive correlation between the ground truth and the predicted model ranking. The unified approach also captures more significant ranking variation in the non-natural image / non-classification benchmarks.

Table 10: **LOVM Model Prediction Ablation.** Here, we ablate all the different scores used in our baselines for mean per-class recall prediction. We separated the text classification (C) base scores, and the granularity-based scores that quantify inter- and intra-class similarity. a_{IN} - Imagenet Accuracy, ϕ_{fisher} - Fisher criterion, text-f1 - caption dataset f1-score, text-acc1 - text top-1 accuracy, γ_{syn} - Synonym Consistency score, φ_{sil} - Silhouette score, ρ_{disp} - Class Dispersion score.

	Scores								Metrics
	Row ID	a_{IN}	text-f1	text-acc1	γ_{syn}	ρ_{disp}	φ_{sil}	ϕ_{fisher}	$L_1 (\downarrow)$
	1	✓	×	×	×	×	×	×	0.228
	2	×	✓	×	×	×	×	×	0.182
	3	×	×	✓	×	×	×	×	0.183
	4	×	×	×	✓	×	×	×	0.179
	5	×	×	×	×	✓	×	×	0.205
	6	×	×	×	×	×	✓	×	0.232
	7	×	×	×	×	×	×	✓	0.175
	8	✓	✓	×	×	×	×	×	0.196
	9	✓	×	✓	×	×	×	×	0.190
	10	✓	×	×	✓	×	×	×	0.225
	11	✓	×	×	×	✓	×	×	0.218
	12	✓	×	×	×	×	✓	×	0.228
	13	✓	×	×	×	×	×	✓	0.177
	14	×	✓	✓	×	×	×	×	0.182
	15	×	✓	×	✓	×	×	×	0.192
	16	×	✓	×	×	✓	×	×	0.191
	17	×	✓	×	×	×	✓	×	0.188
	18	×	✓	×	×	×	×	✓	0.165
	19	×	×	✓	✓	×	×	×	0.190
	20	×	×	✓	×	✓	×	×	0.190
	21	×	×	✓	×	×	✓	×	0.187
	22	×	×	✓	×	×	×	✓	0.162
	23	×	×	×	✓	✓	×	×	0.214
	24	×	×	×	✓	×	✓	×	0.222
	25	×	×	×	✓	×	×	✓	0.159
	26	×	×	×	×	✓	✓	×	0.151
	27	×	×	×	×	✓	×	✓	0.177
	28	×	×	×	×	×	✓	✓	0.181
	29	✓	✓	✓	×	×	×	×	0.197
	30	✓	✓	×	✓	×	×	×	0.203
	31	✓	✓	×	×	✓	×	×	0.196
	32	✓	✓	×	×	×	✓	×	0.195
	33	✓	×	✓	×	×	×	✓	0.164
	34	✓	×	✓	✓	×	×	×	0.203
	35	✓	×	✓	×	✓	×	×	0.196
	36	✓	×	✓	×	×	✓	×	0.194
	37	✓	×	✓	×	×	×	✓	0.163
	38	✓	×	×	✓	✓	×	×	0.227
	39	✓	×	×	✓	×	✓	×	0.232
	40	✓	×	×	✓	×	×	✓	0.164
	41	✓	×	×	×	✓	✓	×	0.156
	42	✓	×	×	×	✓	×	✓	0.177
	43	×	✓	×	×	×	✓	✓	0.179
	44	×	✓	✓	✓	×	×	×	0.191
	45	×	✓	✓	×	×	×	×	0.192
	46	×	✓	✓	×	×	✓	×	0.191
	47	×	✓	×	×	×	×	✓	0.172
	48	×	✓	✓	✓	×	×	×	0.197
	49	×	✓	×	✓	×	✓	×	0.197
	50	×	✓	×	✓	×	×	✓	0.162
	51	×	✓	×	×	✓	✓	×	0.155
	52	×	✓	×	×	×	×	✓	0.171
	53	×	✓	×	×	×	✓	✓	0.176
	54	×	×	✓	✓	×	×	×	0.194
	55	×	×	✓	✓	×	✓	×	0.192
	56	×	×	✓	×	×	×	✓	0.159
	57	×	×	✓	×	✓	✓	×	0.153
	58	×	×	✓	×	×	×	✓	0.169
	59	×	×	✓	×	×	✓	✓	0.173
	60	×	×	×	✓	✓	✓	×	0.145
	61	×	×	×	✓	✓	×	✓	0.164
	62	×	×	×	×	×	✓	✓	0.164
	63	×	×	×	×	✓	✓	✓	0.159
	64	✓	✓	✓	✓	×	×	×	0.206

	Scores								Metrics
	Row ID	a_{IN}	text-f1	text-acc1	γ_{syn}	ρ_{disp}	φ_{sil}	ϕ_{fisher}	$L_1 (\downarrow)$
	65	✓	✓	✓	×	✓	×	×	0.200
	66	✓	✓	✓	×	×	×	×	0.199
	67	✓	✓	✓	×	×	×	✓	0.170
	68	✓	✓	×	✓	×	×	×	0.209
	69	✓	✓	×	✓	×	×	×	0.206
	70	✓	✓	×	✓	×	×	✓	0.168
	71	✓	✓	×	×	×	×	×	0.160
	72	✓	✓	×	×	×	×	✓	0.169
	73	✓	✓	×	×	×	×	✓	0.171
	74	✓	×	✓	✓	×	×	×	0.207
	75	✓	×	✓	✓	×	×	×	0.205
	76	✓	×	✓	✓	×	×	✓	0.166
	77	✓	×	✓	×	×	×	×	0.161
	78	✓	×	✓	×	×	×	✓	0.170
	79	✓	×	✓	×	×	×	✓	0.171
	80	✓	×	×	✓	✓	✓	×	0.152
	81	✓	×	×	✓	✓	×	✓	0.166
	82	✓	×	×	×	×	✓	✓	0.173
	83	✓	×	×	×	×	✓	✓	0.163
	84	×	✓	✓	✓	✓	×	×	0.193
	85	×	✓	✓	✓	×	×	×	0.197
	86	×	✓	✓	✓	×	×	✓	0.170
	87	×	✓	✓	×	×	×	×	0.160
	88	×	✓	✓	×	×	×	✓	0.180
	89	×	✓	✓	×	×	✓	✓	0.182
	90	×	✓	×	✓	✓	×	×	0.156
	91	×	✓	×	✓	✓	×	✓	0.172
	92	×	✓	×	✓	×	×	✓	0.176
	93	×	✓	×	×	✓	✓	✓	0.164
	94	×	×	✓	✓	✓	✓	×	0.155
	95	×	×	✓	✓	✓	×	✓	0.171
	96	×	×	✓	✓	×	✓	✓	0.172
	97	×	×	✓	×	✓	✓	✓	0.162
	98	×	×	×	×	✓	✓	✓	0.151
	99	✓	✓	✓	✓	✓	×	×	0.211
	100	✓	✓	✓	✓	×	×	×	0.203
	101	✓	✓	✓	✓	×	×	✓	0.171
	102	✓	✓	✓	×	×	×	✓	0.163
	103	✓	✓	✓	×	✓	×	×	0.176
	104	✓	✓	✓	×	×	✓	✓	0.178
	105	✓	✓	×	✓	×	×	×	0.162
	106	✓	✓	×	✓	×	×	✓	0.176
	107	✓	✓	×	✓	×	×	✓	0.177
	108	✓	✓	×	×	✓	✓	✓	0.171
	109	✓	×	✓	✓	✓	✓	×	0.162
	110	✓	×	✓	✓	✓	×	✓	0.174
	111	✓	×	✓	✓	×	✓	✓	0.177
	112	✓	×	✓	×	✓	✓	✓	0.171
	113	✓	×	×	✓	✓	✓	✓	0.165
	114	×	✓	✓	✓	✓	×	×	0.159
	115	×	✓	✓	✓	✓	×	✓	0.178
	116	×	✓	✓	✓	×	✓	✓	0.181
	117	×	✓	✓	×	✓	✓	✓	0.168
	118	×	×	×	✓	✓	✓	✓	0.164
	119	×	×	✓	✓	✓	✓	✓	0.162
	120	✓	✓	✓	✓	✓	×	×	0.163
	121	✓	✓	✓	✓	✓	×	×	0.180
	122	✓	✓	✓	✓	×	✓	✓	0.181
	123	✓	✓	✓	×	×	✓	✓	0.172
	124	✓	✓	×	✓	✓	✓	✓	0.171
	125	✓	×	✓	✓	✓	✓	✓	0.171
	126	×	✓	✓	✓	✓	✓	✓	0.167
	127	✓	✓	✓	✓	✓	✓	✓	0.174

C.4 Domain Shift Experiment

An obvious obstacle to text-based model performance prediction methods is the difficulty in describing distribution shifts. For example, VLMs evaluated on ImageNet and ImageNet-v2 will get the same text-predicted accuracy while the actual performance differs. Meanwhile, for some domain shifts - like ImageNet and ImageNet sketch - this shift can be described via text. We want to evaluate how capable text-only methods are at estimating the dataset difficulty under such shifts and compare them to well-accepted image-based approaches.

Dataset Description Similarity. We extract each dataset’s description from either the abstract or introduction section of the original manuscript. Subsequently, we extract the text embeddings for all dataset descriptions using a pre-trained CLIP model. We then compute the cosine similarity

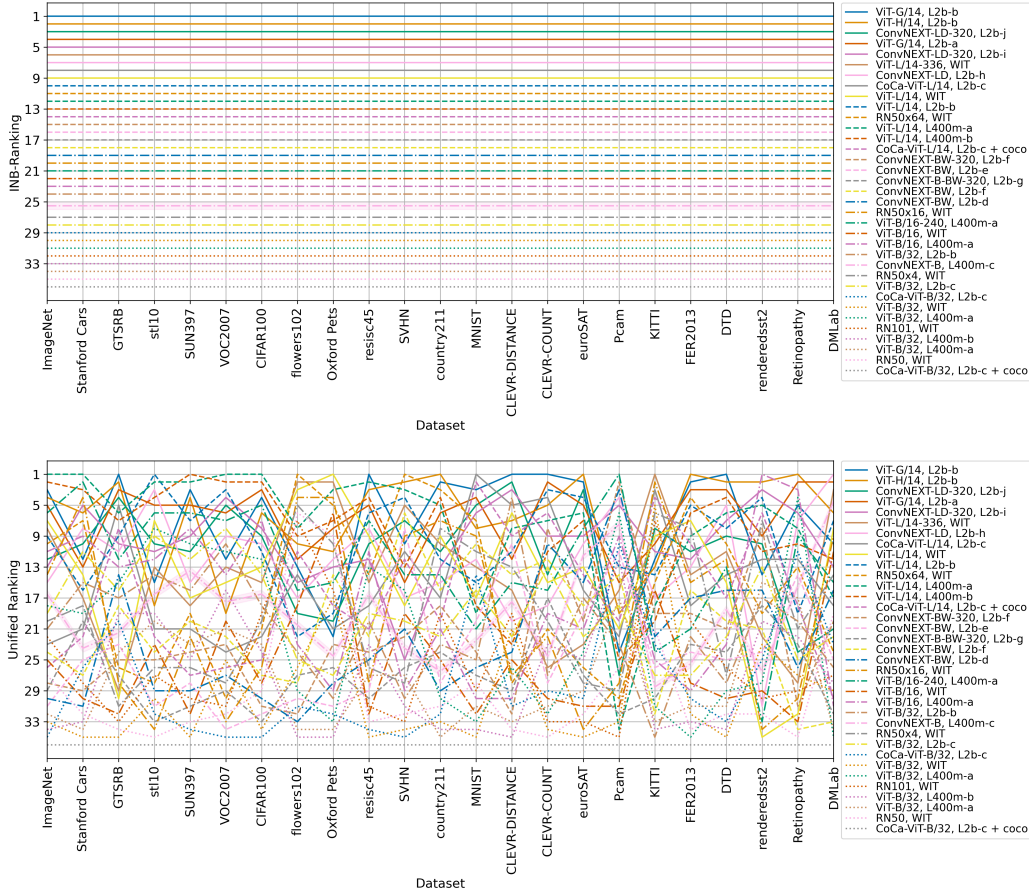


Figure 9: **Raw Model Ranking.** (top) ImageNet benchmark approach assumes the same model ranking for all datasets and cannot predict fine-grained model ranking. (bottom) The unified approach can adjust the coarse ImageNet rankings for a more realistic model ranking.

between the descriptions of the downstream datasets to the original pre-training dataset to quantify how different the two datasets are.

Prompt Embedding Similarity. We use the cosine similarity between dataset-specific and generic class prompts to evaluate domain shift. Specifically, based on the original list of class prompts from CLIP, we pick the ones that best describe our target dataset. For instance, for the ImageNet-sketch dataset, we selected prompts such as “A sketch of a {c}” or “A doodle of a {c}”. Then, we use the text encoder from a pre-trained CLIP model to extract embeddings from dataset-specific and generic class prompts and compute the cosine similarity between each pair. We use the mean cosine similarity to measure how similar the target dataset is to the pre-training dataset. The dataset-specific prompts can be found in the following subsection.

Image-Text Embedding. We wanted to compare with widely used dataset difficulty approaches. One common approach is to use the confidence of a model’s prediction to determine a dataset’s difficulty. To do so, we first n images from the target dataset and extract image embeddings for each of the n images. This simulates the scenario where we only have access to n images from the target dataset to estimate model performance, where n is much smaller than the dataset size. Then, we embed the class prompt into text embeddings and compute the prediction logits between each image embedding and class embeddings. Lastly, we compute the *entropy score* Ethayarajh et al. [2021] and *max prediction logit* Feng et al. [2022] to determine dataset difficulty.

Image Embedding Distance. Another common approach is estimating the difference in distribution between the test and train sets Scheidegger et al. [2018]. We, therefore, use the distance between the

target and pre-training image embeddings to quantify dataset difficulty. Similar to the image-text embedding approach, we first sample n images from the target dataset to extract image embedding using a pre-trained CLIP image encoder. Additionally, we sample m images from the pre-training dataset to extract image embeddings. We only sample m examples since these VLMs are typically pre-trained on an internet-scale dataset, which makes it challenging to embed and compute distance measures on the entire pre-training dataset. We then compute the L_2 distances between the target and pre-training datasets. We use *max*, *min* & *mean* L_2 to quantify dataset difficulty.

Datasets. To evaluate the feasibility and effectiveness of each, we use the following variants of ImageNet. Each dataset captures a different distribution shift from the original ImageNet:

- **ImageNet:** The original ImageNet dataset.
- **ImageNet Version 2 (ImageNet-v2):** A new test set for ImageNet sampled a decade later.
- **ImageNet Sketch (ImageNet-s):** A ImageNet test set dataset with sketch-like iamges.
- **ImageNet Rendition (ImageNet-r):** contains art, cartoons, deviantart, graffiti, embroidery, graphics, origami, paintings, patterns, plastic objects, plush objects, sculptures, sketches, tattoos, toys, and video game renditions of ImageNet classes.
- **ImageNet Adversarial (ImageNet-a):** A real-world distribution shift ImageNet dataset with changes in image style, blurriness, camera operation, and geographic location.

We extract descriptions of each dataset from either the abstract or induction section of their original manuscript. The description used for each dataset is as shown here:

- **LAION400m:** *“a dataset with CLIP-filtered 400 million image-text pairs.”*
- **ImageNet:** *“a benchmark in object category classification and detection on hundreds of object categories.”*
- **ImageNet Version 2:** *“three test sets with 10,000 new images each. Importantly, these test sets were sampled after a decade of progress on the original ImageNet dataset.”*
- **ImageNet Adversarial:** *“real-world distribution shift datasets consisting of changes in image style, image blurriness, geographic locations.”*
- **ImageNet Rendition:** *“art, cartoons, DeviantArt, graffiti, embroidery, graphics, origami, paintings, patterns, plastic objects, plush objects, sculptures, sketches, tattoos, toys, and video game renditions of ImageNet classes.”*
- **ImageNet Sketch:** *“a new dataset consisting of sketch-like images, that matches the ImageNet classification validation set in categories and scale”*

The dataset-specific prompts used for the prompt embedding distance metric are listed in Fig. 10.

Evaluation. We use Kendall’s rank correlation (τ) to evaluate our method’s ability to rank the datasets in terms of their difficulties. Since *image-text embedding* and *ImageNet embedding distance* require sampling from the target dataset, we run our evaluation 1,000 times with different samples and compute the average metric. We also compute the standard deviations of the 1,000 run to estimate the variability of random samples.

We show the results of using our strategies to estimate domain shift in Tab 11. Based on the results, it is clear that none of the current methods can capture the dataset difficulty. Furthermore, the variability based on the standard deviation makes our results heavily dependent on the samples drawn from the target dataset, again suggesting these approaches’ limitations.

D Limitations

Our study, while extensive, is not without limitations. Primarily, our focus rests on zero-shot tasks due to the nature of the LOVM’s design. The framework’s primary aim is to determine the best model for a given task when there is **no** access to the downstream task dataset. Under these circumstances, fine-tuning or linear probing is not viable, as they require access to labeled or unlabeled images from the downstream task dataset. If such data were available, the more straightforward approach would

```

# imagenet prompts
imagenet = [
f'a bad photo of a {c}.',
f'a photo of many {c}.',
f'a bright photo of a {c}.',
f'a photo of a clean {c}.',
f'a photo of a dirty {c}.',
f'a photo of my {c}.',
f'a photo of the cool {c}.',
f'a close-up photo of a {c}.',
f'a bright photo of the {c}.',
f'a photo of the dirty {c}.',
f'a photo of the {c}.',
f'a good photo of the {c}.',
f'a photo of one {c}.',
f'a close-up photo of the {c}.',
f'a photo of a {c}.',
f'a photo of the clean {c}.',
f'a photo of a large {c}.',
f'a photo of a nice {c}.',
f'a good photo of a {c}.',
f'a photo of the nice {c}.',
f'a photo of the small {c}.',
f'a photo of the weird {c}.',
f'a photo of the large {c}.',
f'a photo of a cool {c}.',
f'a photo of a small {c}.',
]

# imagenet v2 prompts
imagenet_v2 = [
f'a bad photo of a {c}.',
f'a photo of many {c}.',
f'a bright photo of a {c}.',
f'a photo of a clean {c}.',
f'a photo of a dirty {c}.',
f'a photo of my {c}.',
f'a photo of the cool {c}.',
f'a close-up photo of a {c}.',
f'a bright photo of the {c}.',
f'a photo of the dirty {c}.',
f'a photo of the {c}.',
f'a good photo of the {c}.',
f'a photo of one {c}.',
f'a close-up photo of the {c}.',
f'a photo of a {c}.',
f'a photo of the clean {c}.',
f'a photo of a large {c}.',
f'a photo of a nice {c}.',
f'a good photo of a {c}.',
f'a photo of the nice {c}.',
f'a photo of the small {c}.',
f'a photo of the weird {c}.',
f'a photo of the large {c}.',
f'a photo of a cool {c}.',
f'a photo of a small {c}.',
]

# imagenet-a prompts
imagenet-a = [
f'a bad photo of a {c}.',
f'a bad photo of the {c}.',
f'a cropped photo of the {c}.',
f'a photo of a hard to see {c}.',
f'a photo of a dirty {c}.',
f'a dark photo of the {c}.',
f'a pixelated photo of the {c}.',
f'a cropped photo of a {c}.',
f'a photo of the dirty {c}.',
f'a blurry photo of the {c}.',
f'a photo of a weird {c}.',
f'a blurry photo of a {c}.',
f'a pixelated photo of a {c}.',
f'a photo of the weird {c}.',
]

# imagenet-s prompts
imagenet-s = [
f'a drawing of a {c}.',
f'a doodle of a {c}.',
f'a sketch of a {c}.',
f'a doodle of the {c}.',
f'a sketch of the {c}.',
]

# imagenet-r prompts
imagenet-r = [
f'a sculpture of a {c}.',
f'a rendering of a {c}.',
f'graffiti of a {c}.',
f'a tattoo of a {c}.',
f'the embroidered {c}.',
f'a drawing of a {c}.',
f'the plastic {c}.',
f'a painting of the {c}.',
f'a painting of a {c}.',
f'a sculpture of the {c}.',
f'a plastic {c}.',
f'a rendering of the {c}.',
f'a {c} in a video game.',
f'the origami {c}.',
f'the {c} in a video game.',
f'a origami {c}.',
f'the toy {c}.',
f'a rendition of a {c}.',
f'a cartoon {c}.',
f'art of a {c}.',
f'a sketch of the {c}.',
f'a embroidered {c}.',
f'a plushie {c}.',
f'the cartoon {c}.',
f'the plushie {c}.',
f'graffiti of the {c}.',
f'a toy {c}.',
f'a tattoo of the {c}.',
]

```

Figure 10: **Prompting Templates Examples.** Above can be examples of different prompting templates used in the study. When using a prompting template, the '{c}' character is replaced by the class name.

Table 11: **Dataset difficulty prediction.** Here we evaluate different method’s ability to rank variations of dataset based on their difficulty. Ground truth is based on CLIP’s zero-shot performance on each dataset. We evaluate each method based on Kendall’s rank correlation (τ). IN - ImageNet, V2 - ImageNet-v2, A - ImageNet Adversarial, R - Imagenet Rendition, S - ImageNet Sketch.

Method	Metric	Raw Value					Rank				τ (\uparrow)	
		IN	V2	A	R	S	IN	V2	A	R		S
True Performance	acc (\uparrow)	0.762	0.701	0.771	0.889	0.602	3	4	2	1	5	1.000
Text Sim.	cosine (\uparrow)	0.807	0.808	0.781	0.832	0.786	3	2	5	1	4	0.200
Prompt Embedding Sim.	cosine (\uparrow)	0.820	0.820	0.801	0.808	0.774	1	1	4	3	5	0.105
Image-Text Embedding	entropy (\uparrow)	$10.819 \pm 1.6e-4$	$9.210 \pm 1.5e-4$	$8.922 \pm 1.8e-4$	$10.309 \pm 1.4e-4$	$10.837 \pm 1.4e-4$	2	5	4	3	1	-0.200
Image-Text Embedding	max logits (\uparrow)	0.273 ± 0.032	0.264 ± 0.035	0.252 ± 0.027	0.260 ± 0.028	0.271 ± 0.029	1	3	5	4	2	-0.400
Image Embedding Dist.	min L_2 (\downarrow)	0.768 ± 0.084	0.790 ± 0.090	0.850 ± 0.068	0.796 ± 0.079	0.753 ± 0.093	2	3	5	4	1	-0.600
Image Embedding Dist.	mean L_2 (\downarrow)	1.422 ± 0.013	1.414 ± 0.014	1.412 ± 0.013	0.413 ± 0.014	1.411 ± 0.012	5	4	2	3	1	-0.200
Image Embedding Dist.	max L_2 (\downarrow)	1.099 ± 0.036	1.103 ± 0.041	1.131 ± 0.033	1.089 ± 0.038	1.077 ± 0.033	3	4	5	2	1	-0.200

be to address the conventional transferability problem as detailed in prior works. The ideal scenario we envision for using LOVM is one where a user with minimal technical expertise seeks to conduct a vision task. In this situation, the user can utilize a LOVM method to discern the most suitable model and the relevant classes, enabling them to deploy the model without needing to delve into technical nuances. However, if one possesses data for fine-tuning, conducting a direct evaluation on this small dataset is likely the most accurate course of action. This constraint stems from the fact that LOVM methods cannot make differential predictions without access to the fine-tuning data. Predicting the performance after fine-tuning or linear probing would heavily depend on the correlation between the results pre and post- fine-tuning/linear probing, a scenario we aim to avoid in the design of LOVM. However, previous work has shown some correlation exists, so there may be some transferability to fine-tuned/linear probed models [Wong et al., 2022].

Secondly, as discussed in Sec. C.4, even datasets bearing identical content may encounter a domain shift. Such shifts can be clearly explained in some cases, such as when comparing ImageNet-regular/rendition/sketch, but in others, the shift may be more elusive. For instance, when comparing ImageNet to ImageNet-a, or when class distribution shifts occur, identifying the source of the shift becomes challenging. In these scenarios, LOVM methods might struggle to accurately predict the performance of a VLM, though model selection might be marginally affected.

Finally, while the utility of text-only solutions described in Sec. C.4 warrants continued investigation, it may be necessary to incorporate unlabeled test images to gauge domain shifts. Combining LOVM methods with these image-based evaluations remains a promising area of ongoing research.

E Broader Impacts

Our work simplifies selecting vision-language models (VLMs) for specific tasks, increasing the accessibility of artificial intelligence (AI) applications. However, this accessibility may be a double-edged sword. On the one hand, it could democratize AI applications, allowing smaller entities or independent researchers to utilize AI technologies more effectively. On the other hand, this easy access might also enable malicious entities to deploy harmful applications more readily, posing risks to sectors such as information security and personal privacy.

Moreover, despite our methodology’s efficiencies, it carries the risk of sub-optimal model selection due to inherent limitations. Inaccuracies could lead to inefficient resource allocation or inferior performance in real-world applications, particularly in high-stakes fields such as healthcare or autonomous driving. Overall, while our work contributes to the efficiency and accessibility of AI applications, it highlights the need for vigilance and continuous refinement to mitigate potential negative impacts.

Checklist

1. For all authors...
 - (a) Do the main claims made in the abstract and introduction accurately reflect the paper's contributions and scope? [Yes]
 - (b) Did you describe the limitations of your work? [Yes] See Sec. D
 - (c) Did you discuss any potential negative societal impacts of your work? [Yes] See Sec. E
 - (d) Have you read the ethics review guidelines and ensured that your paper conforms to them? [Yes]
2. If you are including theoretical results...
 - (a) Did you state the full set of assumptions of all theoretical results? [N/A]
 - (b) Did you include complete proofs of all theoretical results? [N/A]
3. If you ran experiments (e.g. for benchmarks)...
 - (a) Did you include the code, data, and instructions needed to reproduce the main experimental results (either in the supplemental material or as a URL)? [Yes] See Supplemental Material for code repository to reproduce all of our results, has the dataset, and even has an evaluation script for future works.
 - (b) Did you specify all the training details (e.g., data splits, hyperparameters, how they were chosen)? [Yes] See Sec. 3 and Sec. B
 - (c) Did you report error bars (e.g., with respect to the random seed after running experiments multiple times)? [N/A]
 - (d) Did you include the total amount of compute and the type of resources used (e.g., type of GPUs, internal cluster, or cloud provider)? [Yes] see Sec. A
4. If you are using existing assets (e.g., code, data, models) or curating/releasing new assets...
 - (a) If your work uses existing assets, did you cite the creators? [Yes] open-clip, and yes, see Sec. 2.2 and throughout the manuscript
 - (b) Did you mention the license of the assets? [N/A] it is open-source and free to use
 - (c) Did you include any new assets either in the supplemental material or as a URL? [Yes] See codebase in supplemental, will be made open-source
 - (d) Did you discuss whether and how consent was obtained from people whose data you're using/curating? [N/A]
 - (e) Did you discuss whether the data you are using/curating contains personally identifiable information or offensive content? [N/A]
5. If you used crowdsourcing or conducted research with human subjects...
 - (a) Did you include the full text of instructions given to participants and screenshots, if applicable? [N/A]
 - (b) Did you describe any potential participant risks, with links to Institutional Review Board (IRB) approvals, if applicable? [N/A]
 - (c) Did you include the estimated hourly wage paid to participants and the total amount spent on participant compensation? [N/A]